Long-term temperature and precipitation trends at the Coweeta Hydrologic Laboratory, Otto, North Carolina, USA

Stephanie H. Laseter, Chelcy R. Ford, James M. Vose and Lloyd W. Swift Jr

ABSTRACT

Coweeta Hydrologic Laboratory, located in western North Carolina, USA, is a 2,185 ha basin wherein forest climate monitoring and watershed experimentation began in the early 1930s. An extensive climate and hydrologic network has facilitated research for over 75 years. Our objectives in this paper were to describe the monitoring network, present long-term air temperature and precipitation data, and analyze the temporal variation in the long-term temperature and precipitation record. We found that over the period of record: (1) air temperatures have been increasing significantly since the late 1970s, (2) drought severity and frequency have increased with time, and (3) the precipitation distribution has become more extreme over time. We discuss the implications of these trends within the context of regional and global climate change and forest health.

Key words | climate, long-term, precipitation, quantile regression, temperature, time series

Stephanie H. Laseter (corresponding author)
Chelcy R. Ford
James M. Vose
Lloyd W. Swift Jr
USDA Forest Service,
Southern Research Station,
Coweeta Hydrologic Lab,
3160, Coweeta Lab Road,
Otto, North Carolina,
USA
E-mail: *slaseter@fs.fed.us*

INTRODUCTION

The Coweeta Hydrologic Laboratory is among the oldest, continuously operating, environmental study sites in North America and is located in the eastern deciduous forest of the southern Appalachian Mountains in North Carolina, USA (Figure 1). The laboratory was established in 1934 to determine the fundamental effects of forest management on soil and water resources and to serve as a testing ground for theories in forest hydrology (Swank & Crossley 1988). To facilitate this, a network of climate and precipitation stations was established across the site (Figure 1, Tables 1 and 2). The research program has since expanded its focus to encompass watershed ecosystem science. The original climate and precipitation network continues to facilitate these studies and serves as the foundation of the long-term data record.

Forested ecosystems are inherently complex and require a long-term perspective to evaluate responses to natural disturbances and management. Long-term climate data can be an especially important part of this perspective, particularly when evaluating watershed responses to pulse and press climatic events. Without long-term datasets that encompass a wide range of conditions, quantifying hydrologic and ecologic thresholds can be challenging, and identifying cyclical trends or changes in key climate variables can be impossible (Moran *et al.* 2008). A comprehensive description and analysis of the first 50 years of the climate data recorded at Coweeta was published in 1988 (Swift *et al.* 1988). In that study, few climate trends were evident. For example, no significant trends in maximum or minimum annual temperatures, or changes in the distribution of precipitation were detected. Since then, in the southeastern USA, the last 25 years have been characterized by marked changes in key climate variables, including increases in precipitation (Karl & Knight 1998; Groisman *et al.* 2004) leading to greater streamflow (Groisman *et al.* 2004), increased minimum temperatures (Portmann *et al.* 2009), especially minimum temperatures in the summer months (Groisman *et al.* 2004), and increased cloud cover (Dai *et al.* 2006). In addition, the variability of precipitation has also changed in the southeastern USA, with increases in extreme precipitation events (Groisman *et al.* 2004) including high intensity rainfall as well as extreme droughts (Karl & Knight 1998). The ability to separate actual changes or significant trends in climatic variables from

doi: 10.2166/nh.2012.067

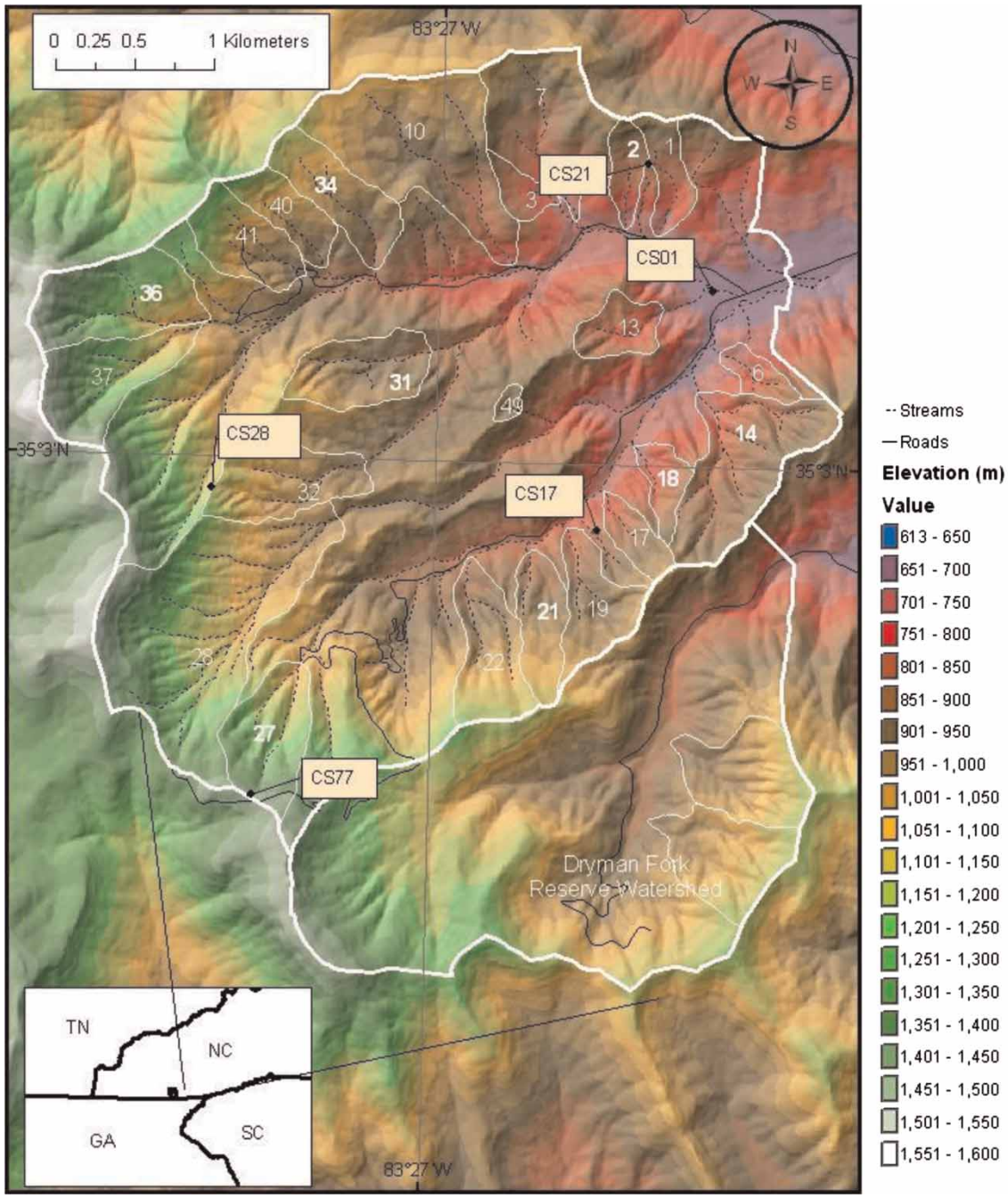

Figure 1 | Elevation gradients and main and sub-watersheds (bold and non-bold white lines, respectively) at Coweeta Hydrologic Lab. Numbers denote reference (bold) and experimental (non-bold) watersheds. Climate stations are identified by white text. Inset: location of Coweeta Basin with respect to southeast USA.

natural variability requires long-term records. Hence, these long-term records are critical for detecting historical changes in climate and they can serve as benchmarks for detecting future change. Our objectives were to provide an update of the climate and precipitation network in the Coweeta Basin, summarize the long-term temperature and precipitation data in the Coweeta Basin, and analyze the temporal variation in these two data series.

Table 1 | Location, elevation and description of climate station network

	Climate station				
	CS01	**CS17**	**CS21**	**CS28**	**CS77**
Location (lat/long)	35°03′37.48 83°25′48.36	35°02′43.33 83°26′14.63	35°03′59.63 83°26′09.12	35°02′47.60 83°27′54.05	35°01′49.27 83°27′37.60
Elevation (m)	685	887	817	1,189	1,398
Aspect	Valley floor	N-facing	S-facing	E-facing	NE-facing
SRG[a]	19	96	17	06	77
RRG[a]	06	96			
Date of first record[b]	8/1934	10/1969	7/1974	5/1985	4/1992
Sensors[c] (units)					
Barometric air pressure (kPa)	✓				
Atmospheric CO_2 concentration (ppm)	✓				
Air temperature (°C) and humidity (%, kPa/kPa)[d]	✓	✓	✓	✓	✓
Photosynthetically active radiation (μmol m^{-2} s^{-1})	✓	✓	✓	✓	✓
Pan evaporation (mm)	✓				
Solar radiation (Ly)	✓				
Soil and litter temperature[e] (°C)		✓	✓	✓	✓
Wind speed (m s^{-1}) and direction (°)	✓	✓	✓	✓	✓

[a]SRG denotes Standard Rain Gage, RRG denotes Recording Rain Gage (See Table 2). Climate stations 21, 28 and 77 have only standard rain gages.
[b]Barometer, photosynthetically active radiation, and digital air relative humidity and temperature sensors added at a later date.
[c]See text for make and model numbers and vendor information of sensors.
[d]Humidity and temperature are recorded with both a hygrothermograph instrument and an HMP45c sensor. Both are located adjacent to National Weather Service maximum, minimum and standard thermometers. Air temperature and humidity readings taken in open field setting as well as within forested cover at all climate stations except CS01.
[e]Only in forest setting.

Table 2 | Location, elevation and date of first record of all paired recording and standard rain gages (RRG and SRG, respectively)

Gage or Station	SRG	Location (lat/long)	Elevation (m)	Date of first record	Aspect
RRG06	19	35°03′37.48/83°25′48.36	687	6/4/1936	Valley bottom
RRG05	02	35°03′37.77/83°27′53.98	1,144	6/4/1936	SE-facing
RRG20	20	35°03′53.37/83°26′29.18	740	11/5/1962	Stream bottom
RRG31	31	35°01′57.89/83°28′05.24	1,366	11/1/1958	High elevation gap
RRG40	13	35°03′44.77/83°27′22.18	961	11/10/1942	S-facing
RRG41	41	35°03′19.11/83°25′43.32	776	5/1/1958	N-facing
RRG45	12	35°02′50.19/83°27′31.11	1,001	6/1/1942	Low elevation gap
RRG55	55	35°02′23.59/83°27′19.32	1,035	11/5/1990	N-facing
RRG96	96	35°02′43.33/83°26′14.63	894	11/1/1943	N-facing

SITE DESCRIPTION

The Coweeta Hydrologic Laboratory is located within the Nantahala Mountain Range of western North Carolina, USA, latitude 35°03′ N, longitude 85°25′ W (Figure 1). The Coweeta Hydrologic Lab is 2,185 ha in area and comprised of two adjacent, east-facing basins. The larger of the two basins (1,626 ha), Coweeta Basin, has been the primary

focus of watershed experimentation. Within the basin, elevations range from 675 to 1,592 m. Climate is classified as maritime, humid temperate (Trewartha 1954; Critchfield 1966).

Historic vegetation patterns in the basin have been influenced by human activity, primarily through small homestead agriculture, both clear-cut and selective logging, the introduction of chestnut blight (*Cryphonectria parasitica)* (Elliott & Hewitt 1997) and hemlock woolly adelgid (*Adelges tsugae*) (Nuckolls *et al*. 2009), and fire management (Hertzler 1936; Douglass & Hoover 1988). The resulting unmanaged forests are relatively mature (~85 years old) oak-hickory (at lower elevations) and northern hardwood forests (at higher elevations) with an increasing component of fire-intolerant species (Elliott & Swank 2008). Bedrock is comprised of granite-gneiss and mica-schist. Soils are immature Inceptisols and older Ultisols and are relatively high in organic matter and moderately acid with both low cation exchange capacity and base saturation.

METHODS

Climate network

Daily temperature and precipitation data have been recorded at the main climate station (CS01) continuously since 1934 (Table 1). In addition to CS01, there are four climate stations across the basin (Table 1). In the 1980s, measurements at each of these stations were expanded in scope and temporal resolution. Each of these stations now continually measures and records (CR10X, Campbell Scientific, Inc., Logan, UT, USA. The following variables every 5 min: temperature and relative humidity in both an open field and forested setting (HMP45c, Campbell Scientific, Logan, UT, USA), photosynthetically active radiation (LI-190-SB, Campbell Scientific), soil and litter temperature under forest cover (107-L, Campbell Scientific) and wind speed and wind direction at canopy height (014A and 024A, MetOne Instruments, Grants Pass, OR, USA). Barometric air pressure (Vaisala CS106, Campbell Scientific), solar radiation (model 8–48, Eppley Lab, Inc., Newport, RI, USA), atmospheric CO_2 concentration (Licor LI-820, Licor, Lincoln, NE, USA) and pan evaporation are measured only at CS01. Data retrieval from the climate network is via wireless remote access. All data recorded to the CR10X datalogger are transmitted via radio frequency (Freewave Technologies, Inc., FGR-115RC, Boulder, CO) from each of the four climate stations to a computer server in the data processing office.

Temperature is recorded at CS01 at 0800 EST daily using a National Weather Service (NWS) maximum, minimum and standard thermometer. Daily minimum and maximum temperatures are recorded and then averaged to determine the average minimum or maximum temperature for the month. In addition, air temperature is digitally recorded on a 5 min increment (CR10X, Campbell Scientific). These values are averaged and hourly maximum, minimum and average temperatures are stored. Weekly absolute maximum and minimum temperatures are recorded at all other climate stations with NWS maximum and minimum thermometers.

Total daily precipitation is collected by an 8 in. Standard Rain Gage (NWS). Rainfall volume and intensity are recorded by Recording Rain Gage (Belfort Universal Recording Rain Gage, Belfort Instrument Co., Baltimore, MD, USA). A network of nine Recording Rain Gages and 12 Standard Rain Gages are located throughout the basin (Table 2). (The use of trade or firm names in this publication is for reader information and does not imply endorsement by the US Department of Agriculture of any product or service.)

Statistical models

To describe the climate data, we present means, extremes, deviations from long-term means, and simple Pearson's correlation coefficients (R) among climate variables and time. To test the hypotheses that mean, maximum and minimum annual air temperature (T, °C) has been increasing in the recent part of the record by fitting a time series intervention models to T data, method is described in detail in Ford *et al*. (2005). Candidate models were a simple level, or a mean level plus a linear increase starting at time t. Each potential starting time in the 1975–1988 range, which was the visual range of the temperature increase, was evaluated sequentially (PROC ARIMA, SAS v9.1, SAS Institute, Inc.). We computed Akaike's

information criterion (AIC) for each model, which is a statistic used to evaluate the goodness of fit and parsimony of a candidate model, with smaller AIC values indicating a better fitting and more parsimonious model than larger values (Johnson & Omland 2004). We used the differences in the AIC values among candidate models with all starting times ($\Delta_i = \mathrm{AIC}_i - \mathrm{AIC}_{\min}$) to compute a relative weight (w_i) for each model relative to all models fit:

$$w_i = \frac{e^{-0.5\Delta_i}}{\sum_{r=1}^{R} e^{-0.5_i\Delta_r}}, \quad (1)$$

with the sum of all w_i equal to 1. The final model selected was the model with the highest w_i (Burnham & Anderson 2002; Johnson & Omland 2004).

We explored whether the high and low ends of the precipitation distribution were changing over time with quantile regression (Cade & Noon 2003). We analyzed linear trends in all quantiles of precipitation (P, mm) to quantify changes to the distribution of annual and monthly precipitation. We used data from the high- and low-elevation standard rain gages (SRG 19 and 31, Table 2) for the entire period of record. Our model predicted the precipitation amount as a function of year, with elevation as a covariate. All models were fit using PROC QUANTREG in SAS (v9.1, SAS Institute, Inc.). If the bootstrapped 95% confidence interval around the estimated coefficient for the quantile overlapped zero, we interpreted this as no significant time trend. To check whether annual precipitation totals from the two gages were consistent over time, we fit a linear model predicting precipitation from SRG 19 as a function of precipitation from SRG 31, year, and the interaction of year and SRG 31 (PROC GLM).

RESULTS

Temperature

Daily and seasonal temperatures do not fluctuate widely (Figure 2). Temperatures are most variable in the winter months. The warmest year on record occurred in 1999

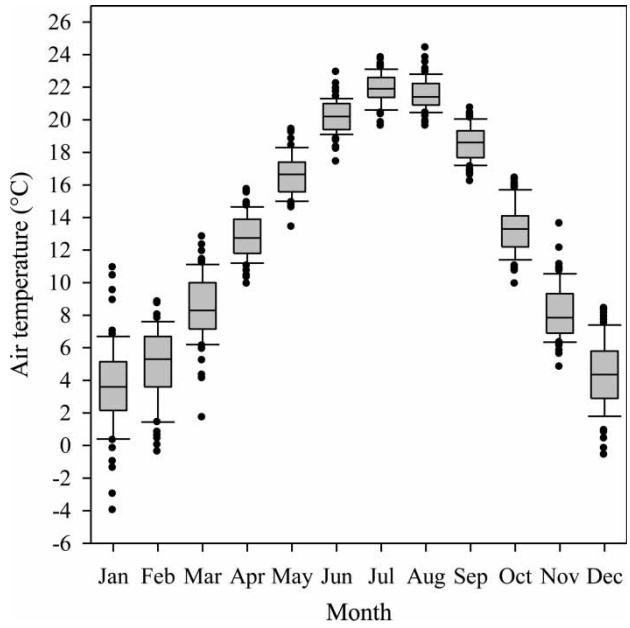

Figure 2 | Monthly mean air temperature at CS01 (see Table 1). Boxes show 75th, 50th, and 25th percentiles. Whiskers show 90th and 10th percentiles. Each outlier (observations outside the 90th and 10th percentiles) is shown.

(average maximum temperature of 21.5 °C). The coldest year on record was 1940 with a minimum of 4.1 °C.

Average annual, maximum and minimum air temperatures at the site have increased significantly relative to the long-term mean (Figure 3). The warming trend is apparent

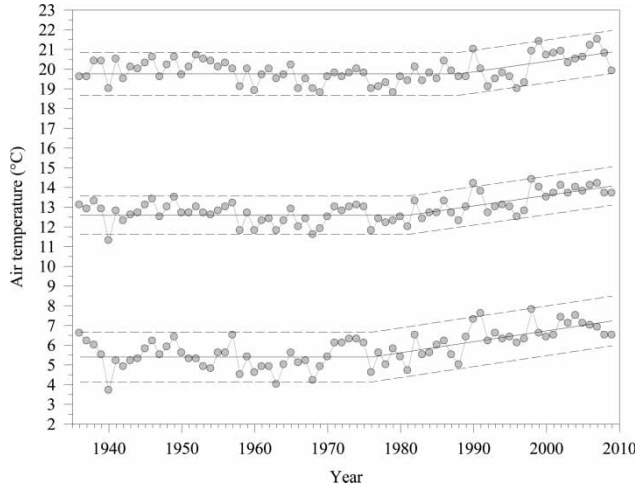

Figure 3 | Long-term average annual, maximum and minimum air temperatures at Coweeta Hydrologic Lab, CS01 (see Table 1). Solid black lines correspond to the modeled mean, with a time series intervention model containing a ramp function at 1981, 1988, and 1976 for average, maximum and minimum data. Dashed lines are the upper and lower 95% confidence intervals about the modeled mean.

in all temperature series (for growing season temperature analysis see Ford *et al.* (2011)), and appeared to begin in the late 1970s to late 1980s. The most parsimonious statistical models indicate a significant increase in average minimum temperatures beginning in 1976 ($w_i = 0.16$), with a rate of increase away from the 5.4 °C long-term mean of 0.5 °C per decade. This same rate of increase occurred in the average annual data series in 1981 ($w_i = 0.13$), and in the annual maximum temperature series in 1988 ($w_i = 0.17$). Average dormant and growing season temperatures also show this trend (data not shown).

Precipitation

Annual precipitation at Coweeta is among the highest in the eastern USA, averaging 1,794 mm (CS01 station, Figure 4 (a)). The basin receives frequent, small, low-intensity storms in all seasons, with the wetter months in late winter and early spring. Fall months are drier (Figure 4 (b)), but generally have larger, more intense tropical storm activity. Elevation has a strong influence on precipitation amount (Figure 4(b)). For example, precipitation at 1,398 m in elevation is 32% (±6% SD) higher than that at 685 m. Although P increases with elevation at the site, P amounts among the rain gages are highly correlated ($0.96 < R^2 < 0.99$), and this relationship is consistent over time (P vs. time $R = 0.02$; no P by year interaction $Pr = 0.73$, $F_{1.73} = 0.12$).

Annual precipitation totals are also becoming more variable over time, with wetter wet years and drier dry years (Figure 5(a) and (b)). Coweeta experienced the wettest year on record in 2009 with a total of 2,375 mm. Only 2 years prior, in 2007, the driest year on record occurred with 1,212 mm. Low quantiles, ~10–20%, had a significant negative slope over time. Higher quantiles, 65–75%, had a significant positive slope over time. This indicates that the low and high ends of the annual precipitation distribution in the basin changed during the period of record. During the wettest years, not all months were wetter; and similarly, during the driest years, not all months were drier. Our results show that the summer months became drier over time, while the fall months became more wet (Figure 5(c)–(f)). In general, most quantiles describing July precipitation declined over time. In September, only the most extreme part (>85%) of the distribution increased over time due to an increase in high intensity, shorter duration storm events, such as tropical storms, as opposed to an increase in the number of storms per month. For example, the number of storms occurring in September did not increase over time ($R = -0.01$, Figure 6(a)), but the percentage of September storms that fell above the 75th percentile (16.5 mm) appears to increase substantially in the latter part of the record (Figure 6(b)). Other fall months became wetter over time, mainly due to increases in the lower percentile storms (data not shown).

In addition to more intense precipitation, recent climate patterns trend toward more frequent periods of prolonged

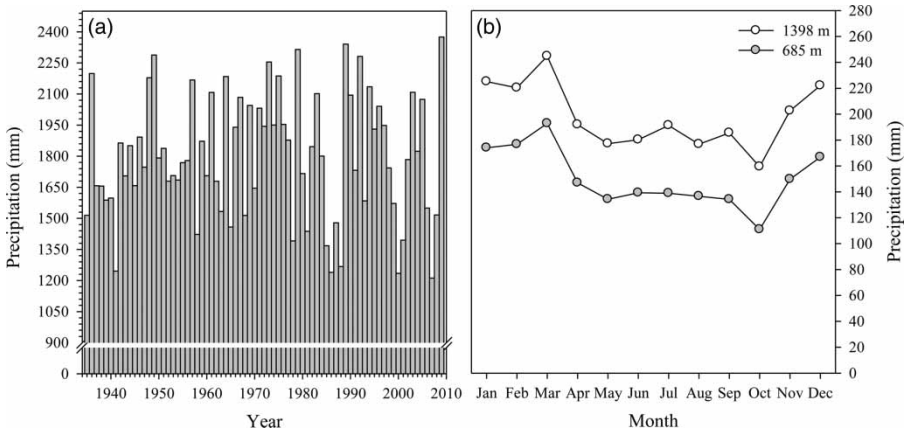

Figure 4 | Total annual precipitation (a) recorded at CS01, and average monthly precipitation (b) at low- and high-elevation stations (see Table 1).

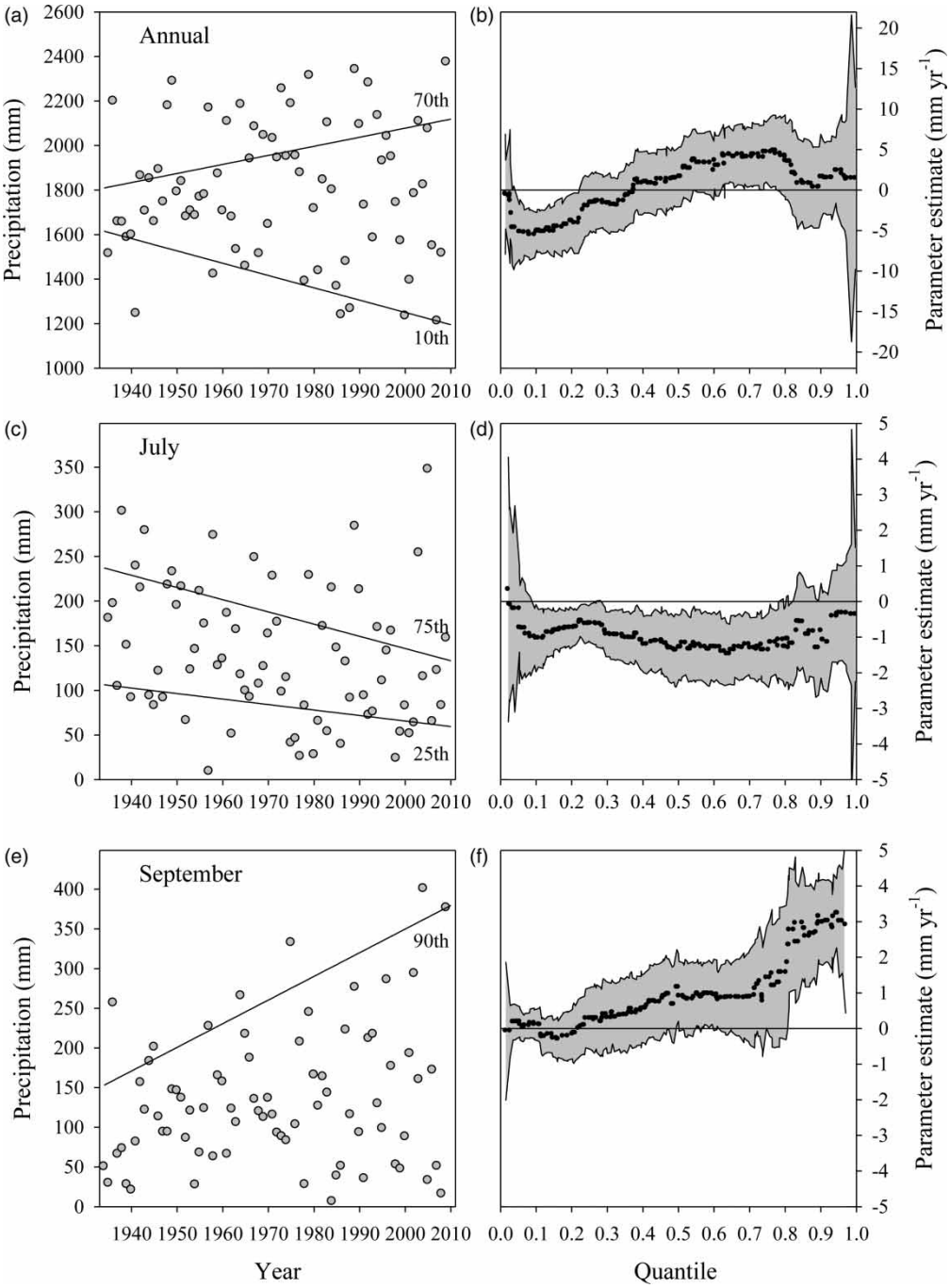

Figure 5 | Annual (a), July (c) and September (e) total precipitation from CS01 (see Table 1). Lines show the modeled *q*th quantile as a function of time. Slopes of all lines shown are significantly different than zero. Panels on right show the modeled estimates (symbols) of the quantile slope conditional on year, for annual (b), July (d) and September (f) precipitation totals. Bootstrapped upper and lower 95% confidence intervals also shown for parameter estimates (grey area).

drought (Figure 7) as inferred by comparing annual totals against the long-term mean. In addition, drought severity (accumulated deficit in precipitation over time) is increasing with time ($R = -0.35$, $t_{0.05,37} = -2.29$, $Pr = 0.01$). Beginning with a severe drought in 1985, a 1,600 mm deficit in rainfall accumulated through 2008.

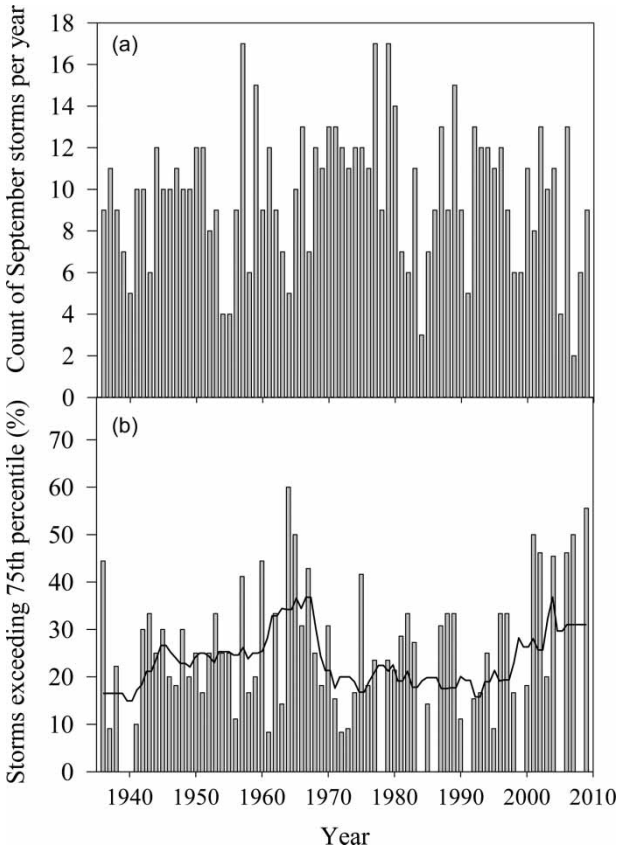

Figure 6 | (a) Number of precipitation events in September for each year in the long-term record, and (b) the percentage of those events that fall above the 75th percentile (16.5 mm). Solid line in (b) is a 10 yr moving average.

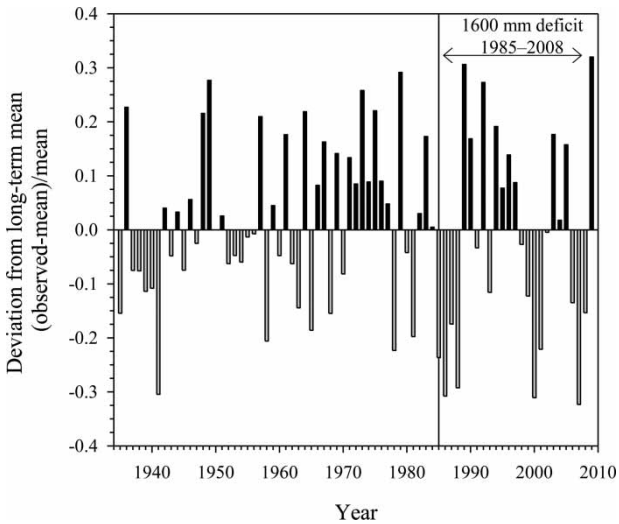

Figure 7 | Deviation of annual precipitation amounts from the long-term mean recorded at CS01 (see Table 1).

DISCUSSION

Climate change

The increased mean annual air temperature (i.e. 0.5 °C per decade) observed since the early 1980s at Coweeta is consistent with other global and regional observations. In the observed climate records, globally, the 20 warmest years have all occurred since 1981 (Peterson & Baringer 2009). Across the USA, a significant warming trend in air temperature also began in the late 1970s to early 1980s (Groisman *et al.* 2004; Peterson & Baringer 2009). This warming trend is predicted to continue; ensemble atmosphere-ocean general circulation models (AOGCMs) predict that by the early 21st century (2030), southeastern US air temperatures will increase at a rate of 0.5 °C per decade (IPCC 2007). Causes for the increases in air temperature include both natural (i.e. surface solar radiation) and anthropogenic (e.g. ozone and CO_2 concentrations) sources, and potential interactions of sources (IPCC 2007). For example, as aerosols increase, surface solar radiation is reduced (i.e. global dimming), which decreases surface temperatures (Wild 2009). One explanation of the lack of significant warming in the 1950–1980 period, followed by the rapid warming in the last 25 years, is that the lower surface solar radiation in the former period masked the warming trend, while the higher surface solar radiation in the latter period apparently accelerated warming (Wild 2009). Although cause and effect is difficult to establish, the timing of increased surface solar radiation is coincident with the passage and implementation of the 1977 Clean Air Act (CAA) and the 1990 CAA Amendments in the USA, which have been quite effective at reducing anthropogenic aerosols (Streets *et al.* 2006). Similar to our hypothesis here, over Europe a 60% reduction in aerosols has been linked to the 1 °C increase in surface temperature since the 1980s due to impacts on shortwave and long-wave forcing (Philipona *et al.* 2009).

Precipitation is increasing in the southeast, similar to what we observed in the Coweeta Basin (Karl & Knight 1998; Groisman *et al.* 2004). These increases in precipitation have translated to increases in streamflow according to long-term US Geological Survey streamflow data (Karl & Knight

1998; Lins & Slack 1999; IPCC 2007). Recent trends in eastern US precipitation, and specifically those in the Coweeta Basin, have been linked to regular patterns in the North Atlantic Oscillation (Riedel 2006a, b). A trend in drier summers since the 1980s has occurred for the southeast (Groisman *et al.* 2004; Angert *et al.* 2005). Simultaneously, a trend in wetter fall months has also occurred (Groisman *et al.* 2004). Our findings in the Coweeta Basin are consistent with both of these larger-scale regional patterns. Whether the trend of increasing precipitation will continue for the region in a warmer, higher-CO_2 scenario is uncertain. Most AOGCMs do not agree on the predicted change in direction of future precipitation for the southern Appalachians and southeast USA, e.g. wetter vs. drier (IPCC 2007).

Many regions of the USA have experienced an increased frequency of precipitation extremes, droughts and floods over the last 50 years (Easterling *et al.* 2000; Groisman *et al.* 2004; Huntington 2006; IPCC 2007). As the climate warms in most AOGCMs, the frequency of extreme precipitation events increases across the globe, resulting in an intensification of the hydrologic cycle (Huntington 2006). For example, the upper 99th percentile of the precipitation distribution is predicted to increase by 25% with a doubling of CO_2 concentration (Allen & Ingram 2002). The lower end of the precipitation distribution is also predicted to change. Forecasts of the drought extent over the next 75 years show that the proportion of land mass experiencing drought will double from 15 to 30% (Burke *et al.* 2006). For example, with a doubling in the peak CO_2 concentration, dry season precipitation is expected to decline irreversibly on average by 15% on most land masses (Solomon *et al.* 2009). The timing and spatial distribution of extreme precipitation events are among the most uncertain aspects of future climate scenarios, however (Karl *et al.* 1995; Allen & Ingram 2002). Our results show that the extremes of the annual precipitation distribution are increasing in magnitude, with recent increases in the frequency of drought, and wetter wet years and drier dry years. We have observed the most extreme precipitation changes in the fall months, with increases in intense rainfall in September in particular. This is partly associated with precipitation generated from tropical storm events. However, a wetter fall season is also being observed due to an increase in the low percentile rain events in November (Ford *et al.* 2011).

Effects on forest function and health

Observed changes in temperature and precipitation distributions that have occurred both locally and regionally have significantly affected forest function and health. The eastern USA has experienced an earlier onset in spring due to rising temperatures (Czikowsky & Fitzjarrald 2004), which has increased spring forest evapotranspiration (Czikowsky & Fitzjarrald 2004) and growth (Nemani *et al.* 2003; McMahon *et al.* 2010). However, the increase in spring growth has been largely offset by drier summers in the southeast (Angert *et al.* 2005), and areas with observed sustained increases in forest growth over time have been those in the northeast (McMahon *et al.* 2010) and at the highest elevations (Salzer *et al.* 2009), where temperatures are more limiting than water, and the tropics (Nemani *et al.* 2003), where radiation is the primary limiting factor.

Whether forest productivity is experiencing recent increases concomitant with temperature increase in the Coweeta Basin has not yet been reported. The effects of extreme events, most notably drought, have had a more dramatic effect on forest health and forest species composition than the trends in temperature. Native insect outbreaks, e.g. southern pine beetle (*Dendroctonus frontalis*), are triggered by drought. The successive droughts in the 1980s and late 1990s caused widespread southern pine beetle infestations in Coweeta watersheds, and throughout the southern Appalachians. As a result of these outbreaks, a decrease in pitch pine (*Pinus rigida*) stands and increased canopy gap area due to dead or dying snags (Clinton *et al.* 1993; Vose & Swank 1994; Kloeppel *et al.* 2003) occurred. The growth of eastern white pine (*Pinus strobus*) has also been significantly reduced by drought (Vose & Swank 1994; McNulty & Swank 1995).

Deciduous hardwood ecosystems have also been impacted by droughts. For example, accelerated mortality of oaks in the red oak group (especially *Quercus coccinea*) occurred during the successive droughts in the 1980s and late 1990s, and interestingly, larger trees were more vulnerable than smaller trees (Clinton *et al.* 1993). The earliest reports of drought in the area in the 1920s also noted that oak mortality was higher than other deciduous tree species (Hursh & Haasis 1931). Growth rate data for oaks

in the 1980–1990 period showed comparable growth rates during wet and dry periods, suggesting either deep rooting and access to stored water in the deep soils at Coweeta (Kloeppel *et al.* 2003), or highly conservative gas exchange in both wet and dry periods (Bush *et al.* 2008; Ford *et al.* 2010).

SUMMARY AND CONCLUSIONS

Analysis of 75 years of climate data at the Coweeta Hydrologic Laboratory has revealed a significant increase in air temperatures since the late 1970s, an increase in drought severity and frequency, and a more extreme precipitation distribution. Cause and effect are difficult to establish, but these patterns are consistent with observations throughout the southeastern USA that suggest linkages between reduced aerosols and temperature patterns, and linkages between the North Atlantic Oscillation and increased precipitation variability. Similar patterns are predicted with AOGCMs under climate change and this recent variability in the observed record may be providing a glimpse of future climatic conditions in the southern Appalachian. Based on observed ecosystem responses to climate variability over the past 20 years, we anticipate significant impacts on ecosystem structure and function.

Climate change during the 21st century is predicted to include novel climates – combinations of seasonal temperature and precipitation that have no historical or modern counterpart (Williams *et al.* 2007). In the USA, the southeastern region is predicted to be the most susceptible to novel climates (Williams & Jackson 2007; Williams *et al.* 2007). Detecting ecosystem change, including ecological 'surprises', will require long-term data from monitoring networks and studies (Lindenmayer *et al.* 2010), such as those presented here from the Coweeta Hydrologic Laboratory.

ACKNOWLEDGEMENTS

This study was supported by the United States Department of Agriculture Forest Service, Southern Research Station, and by NSF grants DEB0218001 and DEB0823293 to the Coweeta LTER program at the University of Georgia. Any opinions, findings, conclusions, or recommendations expressed in the material are those of the authors and do not necessarily reflect the views of the National Science Foundation or the University of Georgia. We acknowledge the support of many individuals, past and present, including Wayne Swank, Charlie L. Shope, Charles Swafford, Neville Buchanan, 'Zero' Shope, Bryant Cunningham, Bruce McCoy, Chuck Marshall, Mark Crawford, and Julia Moore as well as the long-term climate and hydrologic data network at the Coweeta Hydrologic Lab.

REFERENCES

Allen, M. R. & Ingram, W. J. 2002 Constraints on future changes in climate and the hydrologic cycle. *Nature* **419**, 224–232.

Angert, A., Biraud, S., Bonfils, C., Henning, C. C., Buermann, W., Pinzon, J., Tucker, C. J. & Fung, I. 2005 Drier summers cancel out the CO_2 uptake enhancement induced by warmer springs. *Proc. Natl. Acad. Sci.* **102**, 10823–10827.

Burke, E. J., Brown, S. J. & Christidis, N. 2006 Modeling the recent evolution of global drought and projections for the twenty-first century with the Hadley Centre Climate Model. *J. Hydrometeorol.* **7**, 1113–1125.

Burnham, K. P. & Anderson, D. R. 2002 *Model Selection and Multimodel Inference: A Practical Information-Theoretic Approach*. Springer-Verlag, New York.

Bush, S. E., Pataki, D. E., Hultine, K. R., West, A. G., Sperry, J. S. & Ehleringer, J. 2008 Wood anatomy constrains stomatal responses to atmospheric vapor pressure deficit in irrigated, urban trees. *Oecologia* **156**, 13–20.

Cade, B. S. & Noon, B. R. 2003 A gentle introduction to quantile regression for ecologists. *Front. Ecol. Environ.* **1**, 412–420.

Clinton, B. D., Boring, L. R. & Swank, W. T. 1993 Canopy gap characteristics and drought influences in oak forests of the Coweeta Basin. *Ecology* **74**, 1551–1558.

Critchfield, H. J. 1966 *General Climatology*. Prentice Hall, Englewood Cliffs, New Jersey, USA.

Czikowsky, M. J. & Fitzjarrald, D. R. 2004 Evidence of seasonal changes in evapotranspiration in eastern US hydrological records. *J. Hydrometeorol.* **5**, 974–988.

Dai, A., Karl, T. R., Sun, B. & Trenberth, K. E. 2006 Recent trends in cloudiness over the United States, a tale of monitoring inadequacies. *Bull. Am. Meteorol. Soc.* **87**, 597–606.

Douglass, J. E. & Hoover, M. D. 1988 Introduction and site description. In: *Ecological Studies, Vol. 66: Forest Hydrology and Ecology at Coweeta* (W. T. Swank & D. A. Crossley, eds). Springer-Verlag, New York, pp. 17–31.

Easterling, D. R., Meehl, G. A., Parmesan, C., Changnon, S. A., Karl, T. R. & Mearns, L. O. 2000 Climate extremes: observations, modeling, and impacts. *Science* **289**, 2068–2074.

Elliott, K. J. & Hewitt, D. 1997 Forest species diversity in upper elevation hardwood forests in the southern Appalachian Mountains. *Castanea* **62**, 32–42.

Elliott, K. J. & Swank, W. T. 2008 Long-term changes in forest composition and diversity following early logging (1919–1923) and the decline of American chestnut (*Castanea dentata*). *Plant Ecol.* **197**, 155–172.

Ford, C. R., Goranson, C. E., Mitchell, R. J., Will, R. E. & Teskey, R. O. 2005 Modeling canopy transpiration using time series analysis: a case study illustrating the effect of soil moisture deficit on *Pinus taeda*. *Agric. Forest Meteorol.* **130**, 163–175.

Ford, C. R., Hubbard, R. M. & Vose, J. M. 2010 Quantifying structural and physiological controls on canopy transpiration of planted pine and hardwood stand species in the southern Appalachians. *Ecohydrology* **4**, 183–195.

Ford, C. R., Laseter, S. H., Swank, W. T. & Vose, J. M. 2011 Can forest management be used to sustain water-based ecosystem services in the face of climate change? *Ecol. Appl.* **21**, 2049–2067.

Groisman, P. Y., Knight, R. W., Karl, T. R., Easterling, D. R., Sun, B. & Lawrimore, J. H. 2004 Contemporary changes of the hydrological cycle over the contiguous United States: trends derived from *in situ* observations. *J. Hydrometeorol.* **5**, 64–85.

Hertzler, R. A. 1936 *History of the Coweeta Experimental Forest*. Unpublished report on file at Coweeta Hydrologic Laboratory.

Huntington, T. G. 2006 Evidence for intensification of the global water cycle: review and synthesis. *J. Hydrol.* **319**, 83–95.

Hursh, C. R. & Haasis, F. W. 1931 Effects of 1925 summer drought on southern Appalachian hardwoods. *Ecology* **12**, 380–386.

IPCC 2007 Contribution of working groups I, II and III to the fourth assessment report of the Intergovernmental panel on climate change. In: *Climate Change 2007: Synthesis Report*, Core Writing Team (R. K. Pachuari & A. Reisinger, eds). Geneva, Switzerland, pp. 104.

Johnson, J. B. & Omland, K. S. 2004 Model selection in ecology and evolution. *Trends Ecol. Evol.* **19**, 101–108.

Karl, T. R. & Knight, R. W. 1998 Secular trends of precipitation amount, frequency, and intensity in the USA. *Bull. Am. Meteorol. Soc.* **79**, 231–241.

Karl, T. R., Knight, R. W. & Plummer, N. 1995 Trends in high-frequency climate variability in the twentieth century. *Nature* **377**, 217–220.

Kloeppel, B. D., Clinton, B. D., Vose, J. M. & Cooper, A. R. 2003 Drought impacts on tree growth and mortality of southern Appalachian forests. In: *Climate Variability and Ecosystem Response at Long-term Ecological Research Sites* (D. Greenland, D. G. Goodin & R. C. Smith, eds). Oxford University Press, New York, NY, pp. 43–55.

Lindenmayer, D. B., Likens, G. E., Krebs, C. J. & Hobbs, R. J. 2010 Improved probability of detection of ecological 'surprises'. *Proc. Natl. Acad. Sci.* 107, 21957–21962.

Lins, H. & Slack, J. R. 1999 Streamflow trends in the United States. *Geophys. Res. Lett.* **26**, 227–230.

McMahon, S. M., Parker, G. G. & Miller, D. R. 2010 Evidence for a recent increase in forest growth. *Proc. Natl. Acad. Sci.* **107**, 3611–3615.

McNulty, S. G. & Swank, W. T. 1995 Wood $\delta^{13}C$ as a measure of annual basal area growth and soil water stress in a *Pinus strobus* forest. *Ecology* **76**, 1581–1586.

Moran, M. S., Peters, D. P. C., McClaran, M. P., Nichols, M. H. & Adams, M. B. 2008 Long-term data collection at USDA experimental sites for studies of ecohydrology. *Ecohydrology* **1**, 377–393.

Nemani, R. R., Keeling, C. D., Hashimoto, H., Jolly, W. M., Piper, S. C., Tucker, C. J., Myneni, R. B. & Running, S. W. 2003 Climate-driven increases in global terrestrial net primary production from 1982 to 1999. *Science* **300**, 1560–1563.

Nuckolls, A., Wurzburger, N., Ford, C. R., Hendrick, R. L., Vose, J. M. & Kloeppel, B. D. 2009 Hemlock declines rapidly with hemlock woolly adelgid infestation: impacts on the carbon cycle of Southern Appalachian forests. *Ecosystems* **12**, 179–190.

Peterson, T. C. & Baringer, M. O. 2009 State of the climate in 2008. *Bull. Am. Meteorol. Soc.* **90**, S1–S196.

Philipona, R., Behrens, K. & Ruckstuhl, C. 2009 How declining aerosols and rising greenhouse gases forced rapid warming in Europe since the 1980s. *Geophys. Res. Lett.* **36**, L02806.

Portmann, R. W., Solomon, S. & Hegerl, G. C. 2009 Spatial and seasonal patterns in climate change, temperatures, and precipitation across the United States. *Proc. Natl. Acad. Sci.* **106**, 7324–7329.

Riedel, M.S. 2006a North Atlantic oscillation influences on climate variability in the Southern Appalachians. *8th Interdisciplinary Solutions for Watershed Sustainability*. Joint Federal Interagency, Reno, NV.

Riedel, M.S. 2006b Atmospheric/oceanic influence on climate in the Southern Appalachians. In: *Proceedings of the Secondary Interagency Conference on Research in the Watersheds*. USDA SRS, Otto, NC, pp. 7.

Salzer, M. W., Hughes, M. K., Bunn, A. G. & Kipfmueller, K. F. 2009 Recent unprecedented tree-ring growth in bristlecone pine at the highest elevations and possible causes. *Proc. Natl. Acad. Sci.* **106**, 20348–20353.

Solomon, S., Plattner, G., Knutti, R. & Friedlingstein, P. 2009 Irreversible climate change due to carbon dioxide emissions. *Proc. Natl. Acad. Sci.* **106**, 1704–1709.

Streets, D. G., Wu, Y. & Chin, M. 2006 Two-decadal aerosol trends as a likely explanation of the global dimming/brightening transition. *Geophys. Res. Lett.* **33**, L15806.

Swank, W. T. & Crossley, D. A. 1988 Introduction and site description. In: *Ecological Studies, Vol. 66: Forest Hydrology and Ecology at Coweeta* (W. T. Swank & D. A. Crossley, eds). Springer-Verlag, New York, pp. 3–16.

Swift, L. W., Cunningham, G. B. & Douglass, J. E. 1988 Climate and hydrology. In: *Ecological Studies, Vol. 66: Forest Hydrology and Ecology at Coweeta* (W. T. Swank & D. A. Crossley, eds). Springer-Verlag, New York, pp. 35–55.

Trewartha, G. T. 1954 *An Introduction to Climate*. Mc-Graw Hill, New York, USA.

Vose, J. M. & Swank, W.T. 1994 Effects of long-term drought on the hydrology and growth of a white-pine plantation in the southern Appalachians. *For. Ecol. Manage.* **64**, 25–39.

Wild, M. 2009 Global dimming and brightening: a review. *J. Geophys. Res.* **114**, D00D16.

Williams, J. W. & Jackson, S. T. 2007 Novel climates, no-analog communities, and ecological surprises. *Front. Ecol. Environ.* **5**, 475–482.

Williams, J. W., Jackson, S. T. & Kutzbach, J. E. 2007 Projected distributions of novel and disappearing climates by 2100 AD. *Proc. Natl. Acad. Sci.* **104**, 5738–5742.

First received 18 April 2011; accepted in revised form 18 August 2011. Available online 22 February 2012

Microclimate moderates plant responses to macroclimate warming

Pieter De Frenne[a,b,1], Francisco Rodríguez-Sánchez[b], David Anthony Coomes[b], Lander Baeten[a,c], Gorik Verstraeten[a], Mark Vellend[d], Markus Bernhardt-Römermann[e,2], Carissa D. Brown[d,f], Jörg Brunet[g], Johnny Cornelis[h], Guillaume M. Decocq[i], Hartmut Dierschke[j], Ove Eriksson[k], Frank S. Gilliam[l], Radim Hédl[m], Thilo Heinken[n], Martin Hermy[o], Patrick Hommel[p], Michael A. Jenkins[q], Daniel L. Kelly[r], Keith J. Kirby[s], Fraser J. G. Mitchell[r], Tobias Naaf[t], Miles Newman[r], George Peterken[u], Petr Petřík[v], Jan Schultz[w], Grégory Sonnier[x], Hans Van Calster[y], Donald M. Waller[x], Gian-Reto Walther[z], Peter S. White[aa], Kerry D. Woods[bb], Monika Wulf[t], Bente Jessen Graae[cc], and Kris Verheyen[a]

[a]Forest and Nature Lab, Ghent University, BE-9090 Gontrode-Melle, Belgium; [b]Forest Ecology and Conservation Group, Department of Plant Sciences, University of Cambridge, Cambridge CB2 3EA, United Kingdom; [c]Terrestrial Ecology Unit, Department of Biology, Ghent University, BE-9000 Ghent, Belgium; [d]Département de biologie, Université de Sherbrooke, Sherbrooke, QC, Canada J1K 2R1; [e]Institute of Botany, University of Regensburg, DE-93053 Regensburg, Germany; [f]Department of Geography, Memorial University, St. John's, NL, Canada A1B 3X9; [g]Southern Swedish Forest Research Centre, Swedish University of Agricultural Sciences, SE-230 53 Alnarp, Sweden; [h]Agency for Nature and Forests, BE-1000 Brussels, Belgium; [i]Edysan (FRE 3498), Centre National de la Recherche Scientifique/Université de Picardie Jules Verne, FR-80037 Amiens Cedex, France; [j]Department of Vegetation and Phytodiversity Analysis, Albrecht-von-Haller-Institute for Plant Sciences, Georg-August-Universität Göttingen, DE-37073 Göttingen, Germany; [k]Department of Ecology, Environment and Plant Sciences, Stockholm University, SE-106 91 Stockholm, Sweden; [l]Department of Biological Sciences, Marshall University, Huntington, WV 25701; [m]Department of Vegetation Ecology, Institute of Botany of the Academy of Sciences of the Czech Republic, CZ-65720 Brno, Czech Republic; [n]Department of Biodiversity Research/Systematic Botany, Institute of Biochemistry and Biology, University of Potsdam, DE-14469 Potsdam, Germany; [o]Department of Earth and Environmental Sciences, Division of Forest, Nature and Landscape, Katholieke Universiteit Leuven, BE-3001 Leuven, Belgium; [p]Alterra Research Institute, Wageningen UR, 6700 AA Wageningen, The Netherlands; [q]Department of Forestry and Natural Resources, Purdue University, West Lafayette, IN 47907; [r]Botany Department and Trinity Centre for Biodiversity Research, School of Natural Sciences, Trinity College Dublin, Dublin 2, Ireland; [s]Department of Plant Sciences, University of Oxford, Oxford OX1 3RB, United Kingdom; [t]Institute of Land Use Systems, Leibniz-ZALF, DE-15374 Müncheberg, Germany; [u]Beechwood House, St. Briavels Common, Lydney GL15 6SL, United Kingdom; [v]Department of Geographic Information Systems and Remote Sensing, Institute of Botany, Academy of Sciences of the Czech Republic, CZ-25243 Průhonice, Czech Republic; [w]US Forest Service, Milwaukee, WI 53203; [x]Department of Botany, University of Wisconsin–Madison, Madison, WI 53706; [y]Research Institute for Nature and Forest, BE-1070 Brussels, Belgium; [z]Species, Ecosystems, Landscapes Division, Federal Office for the Environment FOEN, CH-3003 Bern, Switzerland; [aa]Department of Biology, University of North Carolina at Chapel Hill, Chapel Hill, NC 27599; [bb]Program in Natural Sciences, Bennington College, Bennington, VT 05201; and [cc]Department of Biology, Norwegian University of Science and Technology, NO-7491 Trondheim, Norway

Edited by Harold A. Mooney, Stanford University, Stanford, CA, and approved September 24, 2013 (received for review June 13, 2013)

Recent global warming is acting across marine, freshwater, and terrestrial ecosystems to favor species adapted to warmer conditions and/or reduce the abundance of cold-adapted organisms (i.e., "thermophilization" of communities). Lack of community responses to increased temperature, however, has also been reported for several taxa and regions, suggesting that "climatic lags" may be frequent. Here we show that microclimatic effects brought about by forest canopy closure can buffer biotic responses to macroclimate warming, thus explaining an apparent climatic lag. Using data from 1,409 vegetation plots in European and North American temperate forests, each surveyed at least twice over an interval of 12–67 y, we document significant thermophilization of ground-layer plant communities. These changes reflect concurrent declines in species adapted to cooler conditions and increases in species adapted to warmer conditions. However, thermophilization, particularly the increase of warm-adapted species, is attenuated in forests whose canopies have become denser, probably reflecting cooler growing-season ground temperatures via increased shading. As standing stocks of trees have increased in many temperate forests in recent decades, local microclimatic effects may commonly be moderating the impacts of macroclimate warming on forest understories. Conversely, increases in harvesting woody biomass—e.g., for bioenergy—may open forest canopies and accelerate thermophilization of temperate forest biodiversity.

climate change | forest management | understory | climatic debt | range shifts

Biological signals of recent global warming are increasingly evident across a wide array of ecosystems (1–7). However, the temperature experienced by organisms at ground level (microclimate) can substantially differ from the atmospheric temperature due to local land cover and terrain variation in terms of vegetation structure, shading, topography, or slope orientation (8–15). The daytime or nighttime surface temperature in rough mountain terrain, for instance, can deviate by up to 9 °C from the air temperature (10). Likewise, forest structure creates substantial temperature heterogeneity, with the interior daytime temperature in dense forests being commonly several degrees cooler than in more open habitats during the growing season (12–15). Spatial microclimatic temperature variation can thus be substantial relative to projected changes in average temperature over time, and biotic

Significance

Around the globe, climate warming is increasing the dominance of warm-adapted species—a process described as "thermophilization." However, thermophilization often lags behind warming of the climate itself, with some recent studies showing no response at all. Using a unique database of more than 1,400 resurveyed vegetation plots in forests across Europe and North America, we document significant thermophilization of understory vegetation. However, the response to macroclimate warming was attenuated in forests whose canopies have become denser. This microclimatic effect likely reflects cooler forest-floor temperatures via increased shading during the growing season in denser forests. Because standing stocks of trees have increased in many temperate forests in recent decades, microclimate may commonly buffer understory plant responses to macroclimate warming.

Author contributions: P.D.F., F.R.-S., D.A.C., G.M.D., B.J.G., and K.V. designed research; P.D.F., F.R.-S., L.B., G.V., M.V., M.B.-R., C.D.B., J.B., J.C., G.M.D., H.D., O.E., F.S.G., R.H., T.H., M.H., P.H., M.A.J., D.L.K., K.J.K., F.J.G.M., T.N., M.N., G.P., P.P., J.S., G.S., H.V.C., D.M.W., G.-R.W., P.S.W., K.D.W., M.W., and K.V. performed research; P.D.F., F.R.-S., L.B., G.V., and K.V. analyzed data; and P.D.F., F.R.-S., D.A.C., L.B., M.V., M.B.-R., C.D.B., J.B., J.C., G.M.D., O.E., F.S.G., R.H., T.H., M.H., M.A.J., D.L.K., K.J.K., M.N., G.P., P.P., G.S., H.V.C., D.M.W., P.S.W., K.D.W., B.J.G., and K.V. wrote the paper.

The authors declare no conflict of interest.

This article is a PNAS Direct Submission.

[1]To whom correspondence should be addressed. E-mail: pieter.defrenne@ugent.be.

[2]Present address: Institute of Ecology, Friedrich-Schiller-University Jena, DE-07743 Jena, Germany.

This article contains supporting information online at www.pnas.org/lookup/suppl/doi:10.1073/pnas.1311190110/-/DCSupplemental.

responses to macroclimate warming may be buffered by microclimatic heterogeneity (9–11). It seems likely that microclimates can modulate the large-scale, multispecies, and long-term response of biota to macroclimate warming, but this is currently unverified. Testing this idea will permit incorporation of fine-grained thermal variability into bioclimatic modeling of future species distributions (11, 16), and is particularly relevant to forest understories, which play a key role in vital ecosystem services of forests such as tree regeneration, nutrient cycling, and pollination (17, 18). Additionally, microclimatic buffering might help to explain the lag of community responses to increased temperature that has been reported for several taxa and regions (3, 5, 7).

Temperate forests comprise 16% (5.3 million km^2) of the world's forests (19), and understory plants represent on average more than 80% of temperate forest plant diversity (17). Temperate forests have recently experienced pronounced climate warming, but have also been heavily influenced by other environmental changes. Changing forest management regimes due to altered socioeconomic conditions, but also eutrophication, climate warming, and fire suppression, have resulted in increased tree growth, standing stocks, and densities in many temperate forests of the northern hemisphere (20–25). In Western Europe, for instance, logging and natural losses of tree biomass have been consistently lower than annual growth increments, resulting in an almost doubling of standing stocks of trees per hectare between 1950 and 2000 (21). Hence, forests' powerful influence on terrestrial microclimates raises the intriguing possibility that non-climatic drivers of global change, such as forest canopy closure, might have lowered ground-level temperatures via increased shading, thereby counteracting the effects of macroclimate warming on the forest understory.

Here we compiled plant occurrence data (1,032 species in total) from 1,409 resurveyed vegetation plots in temperate deciduous forests. The plots were distributed across 29 regions of temperate Europe and North America (Fig. 1 *A* and *B*) with an average interval of 34.5 y (range: 12–67 y) between the original and repeated vegetation surveys (Table S1). From these plots, we tested for plant community responses to recent macroclimate warming and assessed the potential role of changes in forest canopy cover in modulating such responses. To quantify possible thermophilization of communities, we inferred the temperature preferences of species from distribution data by means of ecological niche modeling (16) (Fig. 1 *A*–*C*). This method builds on previous use of species' temperature preferences to assess community-level climate-change impacts (3–6). We then calculated the floristic temperature for each plot by sampling from the temperature preference distributions of all species that were present at the time of the surveys. The probability of sampling a temperature for a particular species was determined by the shape of its thermal response curve as estimated by niche modeling. We repeated this resampling procedure 500 times to account for the variability and uncertainty in species' temperature

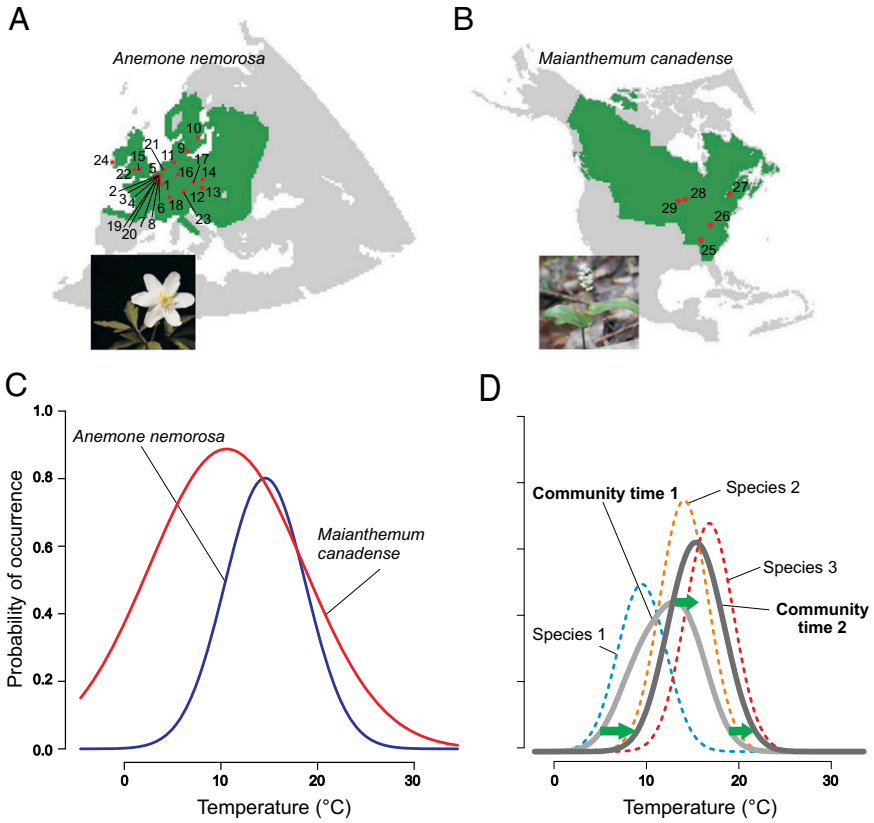

Fig. 1. Estimation of plant thermal response curves and temporal community-level responses to warming. (*A*–*C*) Thermal response curves were estimated from species' current distribution ranges (green areas in maps). The two most frequent understory species in the database are shown as an example: *Anemone nemorosa* from Europe (*A*) and *Maianthemum canadense* from North America (*B*) (Tables S2 and S3). The red dots indicate the locations of the 29 study regions and numbers refer to site descriptions in Table S1. (*D*) Hypothetical community response to warming: the community consists of species 1 and 2 at time 1 and species 2 and 3 at time 2, which results in thermophilization between time 1 and 2 because the more cold-adapted species 1 is lost from the community, and the more warm-adapted species 3 is gained. The green arrows represent the temporal shift of the mean, left tail (fifth percentile) and right tail (95th percentile) of the distribution of floristic temperatures and reflect the degree to which the mean thermophilization increases, cold-adapted species decrease, and warm-adapted species increase, respectively.

preferences (26). Communities with many cold-adapted species will thus have a lower floristic temperature, and vice versa. To assess thermophilization over time, we compared the mean, fifth, and 95th percentiles of the temperature distribution for every plot at the old and recent survey, respectively (Fig. 1*D*). The shift of the mean of the distribution of floristic temperatures (in degrees Celsius per decade) then reflects the mean thermophilization. In contrast, shifts in the tails of the distribution of plot-level floristic temperatures (fifth and 95th percentiles) reflect changes in the occurrence of cold and warm-adapted species, respectively (Fig. 1*D*).

Results and Discussion

Significant community turnover took place over time in the temperate forests we sampled: on average, one-third of the species present in the old surveys has been replaced by other species today; the mean Lennon dissimilarity index (*SI Materials and Methods*) across all plots was 0.69 (95% bootstrapping confidence interval: [0.68, 0.70]), both in Europe (dissimilarity was 0.70 [0.69, 0.71]) and North America (0.65 [0.62, 0.68]). This floristic turnover partly arose from the nonrandom replacement of species in terms of their temperature preferences, illustrated by significant thermophilization both in European and eastern North American forests (Fig. 2*A*). On average, the estimated thermophilization rate was 0.041 °C·decade^{-1} (the range across 10 different modeling methods was 0.027–0.056 °C·decade^{-1}; Table S4). Significant interregional variation was present, with thermophilization rates ranging from +0.83 °C·decade^{-1} (Great Smoky Mountains) to –0.64 °C·decade^{-1} (Ireland). Thermophilization was significantly positive in 20 of 29 regions, significantly negative in eight study regions, and unchanged in one region (Fig. 2*B*).

The overall thermophilization of understory plant communities has been driven by concurrent gains of relatively warm-adapted species and loss of cold-adapted taxa, as revealed by the shifts in the cold (fifth percentile) and warm (95th percentile) ends of the floristic temperature distribution (Fig. 2*C*). In the eastern North American forest plots, however, both warm-adapted and cold-tolerant species have increased (Fig. 2*C*) due to continuous immigration of new species (i.e., overall increase in species richness), which does not occur in the European plots (*SI Results*). The mean thermophilization of understory plant communities that we observe across temperate deciduous forests in two continents expands on earlier findings that mountain vegetation communities are showing increases of lower-altitude species at higher altitudes, leading to novel species assemblages (3, 4, 27). The thermophilization of vegetation is consistent with the warming climate observed across the regions: the mean rise in April-to-September temperatures between the old and recent survey was 0.28 °C·decade^{-1} (Table S1). We found a positive relationship between the thermophilization and the region-specific April-to-September temperature change, indicating higher thermophilization in areas with higher rates of warming (mean slope 0.07, $P < 0.001$; *SI Results*). European and North American temperate deciduous forest vegetation is thus changing as expected by macroclimate warming, but thermophilization lags behind rising temperatures.

We found that local changes in forest canopy cover modulate the thermophilization of vegetation; thermophilization was lowest in forests that became denser, and highest in forests that

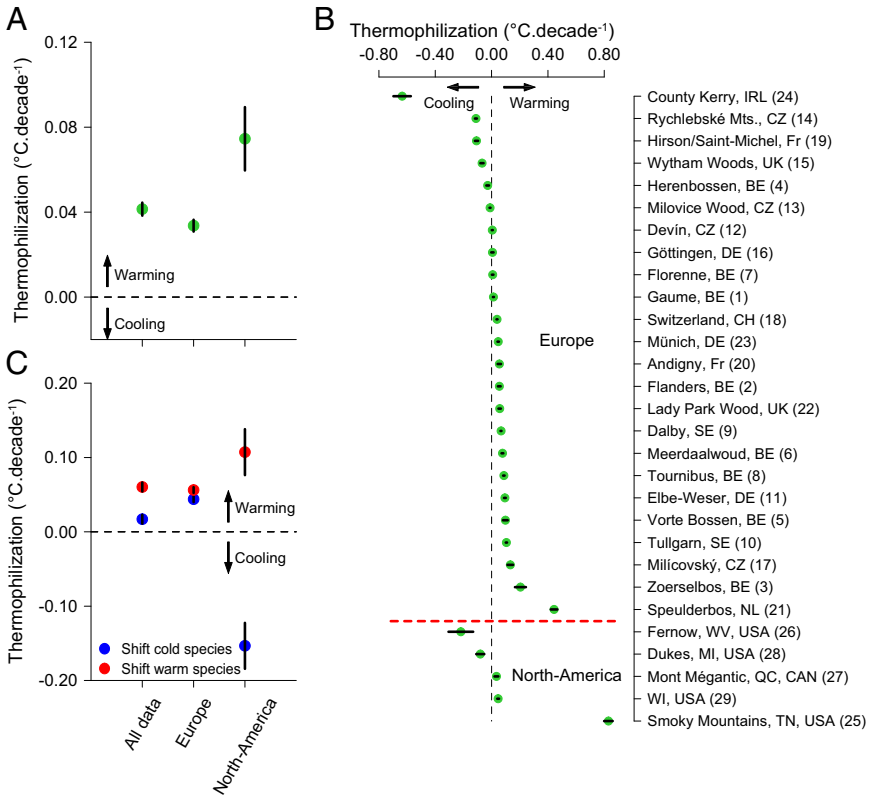

Fig. 2. Thermophilization of temperate forest understories across Europe and North America. (*A* and *B*) Mean thermophilization (positive values denote increases over time) for all data and in European and American forests (*A*) and for the individual regions (*B*). The numbers between brackets refer to the sites in Fig. 1. (*C*) Mean shifts in relatively cold-adapted (blue) and warm-adapted species (red) for all plots, and in Europe and North America. Positive values reflect positive shifts of the left and right tail, i.e., decreases of cold-adapted and increases of warm-adapted taxa, respectively. Error bars denote the 95% confidence intervals based on 500 resampled species' temperature preferences.

became more open over time (Fig. 3*A*). The relationship between forest canopy cover changes and the mean thermophilization was significantly negative (mean slope = –0.0073, $P < 0.001$, range of slopes across 10 different modeling methods –0.0392 to –0.0015; Table S5). Moreover, the increase of warm-adapted species was consistently lower in plots that increased in canopy cover compared with plots that became more open over time, which experienced stronger thermophilization (mean slope = –0.0170, $P < 0.001$, range across 10 different modeling methods –0.0463 to –0.0099). For cold-adapted species, the effects of canopy cover changes were lower and more variable (mean slope = –0.0071, $P < 0.05$, range across 10 different modeling methods –0.0584 to + 0.0083). Thus, cold-adapted taxa responded to a lesser extent to changes in forest canopy cover (Fig. 3*B*). Taken together, these results suggest that recent forest canopy closure in northern-hemispheric temperate forests has buffered the impacts of macroclimate warming on ground-layer plant communities, thus slowing changes in community composition.

Forest canopy closure modulates macroclimatic trends through the effects on local microclimates. Dense tree canopies not only lower ground-layer temperatures but also increase relative air humidity and shade in the understory (12–15). Hence, the reported decrease in light-demanding understory plants in Europe (28) is also congruent with the local environmental effects caused by forest canopy closure. Higher relative humidity in dense forests can also protect forest herbs and tree seedlings from summer drought, decreasing mortality and thus buffering the impacts of large-scale climate change (15, 29). Furthermore, many forest herbs are known to be slow-colonizing species (30). Given the high degree of habitat fragmentation in contemporary landscapes, microclimatic buffering in dense forests may be a critical mechanism to ensure the future conservation of temperate forest plant diversity.

If forest canopy closure attenuates warming in the understory, atmospheric temperatures provide an unrealistic benchmark against which to compare floristic temperatures. Hence, land-use changes such as forest canopy closure could partially explain the lag observed between, for instance, lowland forest plant community composition (3) and temperature trends as measured in weather stations (i.e., above dwarf vegetation in open areas). Instead of accumulating climatic lags, these understory communities could be mostly exploiting the buffering microclimatic effects brought about by canopy closure. Therefore, measuring climate change in the field and identifying the actual climatic lags of biota is crucial to further our understanding of community reordering and future biodiversity conservation in the face of climate change.

In sum, we observed increasing dominance of warm-adapted understory plants across more than 1,400 plots and 29 regions in European and North American temperate deciduous forests. Additionally, our most striking finding is the temporal buffering of the continent-wide response of understory vegetation to macroclimate warming by forest canopy closure. The importance of increased canopy cover in influencing understory biodiversity is particularly relevant in an era when forest management worldwide is confronted with increasing demands for woody biomass, not least as an alternative source of renewable energy (31, 32). In addition, current conservation actions in European forests are regularly directed toward restoring traditional management (e.g., coppicing in ancient forests), resulting in canopy opening. Such actions could not only result in soil nutrient depletion, lower biomass pools, and enhanced soil nitrogen release (28, 31), but also, depending on the sylvicultural system applied, increase temperatures at the forest floor (12–15). Large-scale reopening of the canopy for woody biomass harvesting may thus hasten thermophilization of understory plant communities of temperate forests.

Materials and Methods

Understory Resurveys. We compiled complete species lists of 1,409 rigorously selected (*SI Materials and Methods*) resurveyed vegetation plots in European and North American ancient deciduous forests, and determined forest canopy cover changes (sum of the tree and shrub species' canopy cover) for 854 of the plots (19 regions; Table S1 and Fig. S1). Plots were either permanently marked or semipermanent (i.e., with known coordinates; *SI Materials and Methods*), and plot sizes ranged between 1 and 1,000 m^2 (Table S1). Plot-level changes in canopy cover between the old and recent surveys were quantified as response ratios $\log(cover_{recent}/cover_{old})$.

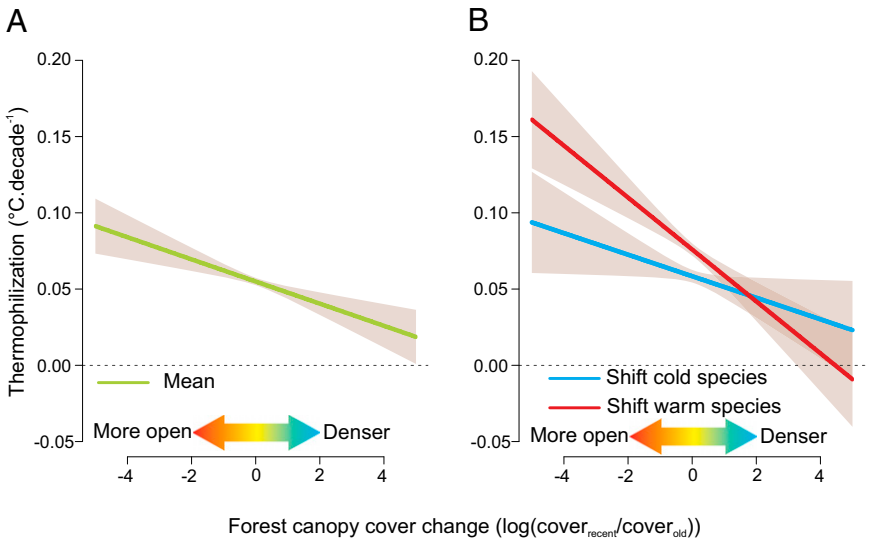

Fig. 3. Forest canopy closure modulates understory thermophilization. (*A*) Relationship between forest canopy cover change and mean thermophilization of understory plant communities in temperate European and North American forests. (*B*) Relationship between forest canopy cover change and decreases of cold-adapted species (expressed by the shift of the left tail of the plot-level distribution of floristic temperatures, blue) and increases of warm-adapted species (expressed by the shift of the right tail of the plot-level distribution of floristic temperatures, red). Relationships result from mixed-effect models for each of 500 samples; shaded areas denote 95% confidence intervals based on those samples. These results are mainly based on the European data (Table S1).

Calculation of Thermophilization. We calculated the thermophilization for each plot by sampling from the inferred temperature preference distributions of the species present (Fig. 1). The long-term mean temperature and precipitation in the growing season (April to September; Fig. S2) were used to estimate species' thermal response curves by means of ecological niche modeling (16). To account for variability and uncertainty in species' thermal preferences and niche widths (26), the distribution of plot-level floristic temperatures at each survey was constructed by resampling 500 times from species' thermal response curves. The mean thermophilization per plot was quantified as the difference between the mean floristic temperature (in degrees Celsius) between the recent and original survey, divided by the time interval (in decades) between the two surveys. In addition, we determined the contribution of the loss of cold-adapted and the gain of warm-adapted species to the thermophilization patterns by quantifying the shifts in the left and right tails (fifth and 95th percentiles, respectively) of the plot-level distribution of floristic temperatures (Fig. 1*D* and Figs. S3 and S4).

Forest Cover and Temperature Change vs. Thermophilization. The relationships between forest canopy cover and temperature changes on the one hand, and thermophilization on the other hand (shifts in the mean, fifth, and 95th percentiles of the distribution of floristic temperatures over time) were assessed using mixed-effect models with "study region" as a random-effect term for each of the 500 resampled species' temperature preferences. Sensitivity analyses revealed that excluding precipitation, applying various climatic periods, study area extents, and modeling approaches, and randomly removing subsets of species resulted in consistent results (see *SI Materials and Methods* for a detailed account of the methods and *SI Results* for supporting results).

ACKNOWLEDGMENTS. We thank J. Kartesz and M. Nishino for the American species distribution maps, two anonymous reviewers for valuable comments, and the Research Foundation–Flanders (FWO) for funding the scientific research network FLEUR. Support for this work was provided by FWO Postdoctoral Fellowships (to P.D.F. and L.B.), European Union Seventh Framework Programme FP7/2007-2013 Grant 275094 (to F.R.-S.), the Natural Sciences and Engineering Research Council of Canada (M.V. and C.D.B.), and long-term research development project RVO 67985939 (to R.H. and P.P.).

1. Walther GR, et al. (2002) Ecological responses to recent climate change. *Nature* 416(6879):389–395.
2. Parmesan C (2006) Ecological and evolutionary responses to recent climate change. *Annu Rev Ecol Evol Syst* 37:637–669.
3. Bertrand R, et al. (2011) Changes in plant community composition lag behind climate warming in lowland forests. *Nature* 479(7374):517–520.
4. Gottfried M, et al. (2012) Continent-wide response of mountain vegetation to climate change. *Nature Clim Change* 2(2):111–115.
5. Devictor V, et al. (2012) Differences in the climatic debts of birds and butterflies at a continental scale. *Nature Clim Change* 2(2):121–124.
6. Cheung WWL, Watson R, Pauly D (2013) Signature of ocean warming in global fisheries catch. *Nature* 497(7449):365–368.
7. Dullinger S, et al. (2012) Extinction debt of high-mountain plants under twenty-first-century climate change. *Nature Clim Change* 2(8):619–622.
8. Kraus G (1911) *Soil and Climate in a Small Space* (Fischer, Jena, East Germany), German.
9. Dobrowski SZ (2011) A climatic basis for microrefugia: The influence of terrain on climate. *Glob Change Biol* 17(2):1022–1035.
10. Scherrer D, Körner C (2010) Infra-red thermometry of alpine landscapes challenges climatic warming projections. *Glob Change Biol* 16(9):2602–2613.
11. Lenoir J, et al. (2013) Local temperatures inferred from plant communities suggest strong spatial buffering of climate warming across Northern Europe. *Glob Change Biol* 19(5):1470–1481.
12. Geiger R, Aron RH, Todhunter P (2009) *The Climate Near the Ground* (Rowman & Littlefield, Plymouth, UK), 7th Ed.
13. Chen J, et al. (1999) Microclimate in forest ecosystem and landscape ecology. *Bioscience* 49(4):288–297.
14. Norris C, Hobson P, Ibisch PL (2012) Microclimate and vegetation function as indicators of forest thermodynamic efficiency. *J Appl Ecol* 49(3):562–570.
15. von Arx G, Graf Pannatier E, Thimonier A, Rebetez M (2013) Microclimate in forests with varying leaf area index and soil moisture: Potential implications for seedling establishment in a changing climate. *J Ecol* 101(5):1201–1213.
16. Peterson AT, et al. (2011) *Ecological Niches and Geographic Distributions* (Princeton Univ Press, Princeton, NJ).
17. Gilliam FS (2007) The ecological significance of the herbaceous layer in temperate forest ecosystems. *Bioscience* 57(10):845–858.
18. Nilsson MC, Wardle DA (2005) Understory vegetation as a forest ecosystem driver: Evidence from the northern Swedish boreal forest. *Front Ecol Environ* 3(8):421–428.
19. Hansen MC, Stehman SV, Potapov PV (2010) Quantification of global gross forest cover loss. *Proc Natl Acad Sci USA* 107(19):8650–8655.
20. United Nations Economic Commission for Europe/Food and Agricultural Organization (2000) *Forest Resources of Europe, CIS, North America, Australia, Japan and New Zealand (Industrialized Temperate/Boreal Countries).* Geneva Timber and Forest Study Papers (United Nations, New York).
21. Gold S, Korotkov AV, Sasse V (2006) The development of European forest resources, 1950 to 2000. *For Policy Econ* 8(2):183–192.
22. Rautiainen A, Wernick I, Waggoner PE, Ausubel JH, Kauppi PE (2011) A national and international analysis of changing forest density. *PLoS ONE* 6(5):e19577.
23. Luyssaert S, et al. (2010) The European carbon balance. Part 3: Forests. *Glob Change Biol* 16(5):1429–1450.
24. Thomas RQ, Canham CD, Weathers KC, Goodale CL (2010) Increased tree carbon storage in response to nitrogen deposition in the US. *Nat Geosci* 3(1):13–17.
25. McMahon SM, Parker GG, Miller DR (2010) Evidence for a recent increase in forest growth. *Proc Natl Acad Sci USA* 107(8):3611–3615.
26. Rodríguez-Sánchez F, De Frenne P, Hampe A (2012) Uncertainty in thermal tolerances and climatic debt. *Nature Clim Change* 2(9):636–637.
27. Lenoir J, Gégout JC, Marquet PA, de Ruffray P, Brisse H (2008) A significant upward shift in plant species optimum elevation during the 20th century. *Science* 320(5884):1768–1771.
28. Verheyen K, et al. (2012) Driving factors behind the eutrophication signal in understorey plant communities of deciduous temperate forests. *J Ecol* 100(2):352–365.
29. Lendzion J, Leuschner C (2009) Temperate forest herbs are adapted to high air humidity—evidence from climate chamber and humidity manipulation experiments in the field. *Can J Res* 39(12):2332–2342.
30. De Frenne P, et al. (2011) Interregional variation in the floristic recovery of post-agricultural forests. *J Ecol* 99(2):600–609.
31. Schulze ED, Körner C, Law BE, Haberl H, Luyssaert S (2012) Large-scale bioenergy from additional harvest of forest biomass is neither sustainable nor greenhouse gas neutral. *GCB Bioenergy* 4(6):611–616.
32. Tilman D, et al. (2009) Energy. Beneficial biofuels—the food, energy, and environment trilemma. *Science* 325(5938):270–271.

doi:10.1038/nature12914

Supplementary Table 1 | Results by species.

Country	Data ref.	Family	Species	# of trees	Max. tree diam. (cm)	Allom. ref.	Bin 1	Bin 2	Bin 3	Bin 4
Cameroon	51	Achariaceae	Scottellia klaineana	153	70.6	34	+	+		
Cameroon	51	Annonaceae	Annickia chlorantha	106	51.2	34	+			
Cameroon	51	Annonaceae	Xylopia aethiopica	71	53.3	34	+			
Cameroon	51	Combretaceae	Strephonema pseudocola	55	130.7	34	(+)	+		
Cameroon	51	Dichapetalaceae	Tapura africana	57	74.9	34	+			
Cameroon	51	Ebenaceae	Diospyros gabunensis	744	50.4	34	(+)	+	+	
Cameroon	51	Erythropalaceae	Strombosia pustulata	684	46.5	34	+	+		
Cameroon	51	Erythropalaceae	Strombosia scheffleri	119	69.9	34	+			
Cameroon	51	Erythropalaceae	Strombosiopsis tetrandra	230	68.9	34	+			
Cameroon	51	Euphorbiaceae	Dichostemma glaucescens	1771	44.5	34	+			
Cameroon	51	Euphorbiaceae	Discoglypremna caloneura	43	64.9	34	+			
Cameroon	51	Euphorbiaceae	Klaineanthus gaboniae	355	55.7	34	+			
Cameroon	51	Fabaceae	Hymenostegia afzelii	476	44.3	34	+			
Cameroon	51	Fabaceae	Talbotiella eketensis	132	51.2	34	+			
Cameroon	51	Lamiaceae	Vitex grandifolia	80	46.6	34	+			
Cameroon	51	Lamiaceae	Vitex sp.1	48	126.5	34	+			
Cameroon	51	Lauraceae	Hypodaphnis zenkeri	129	91.8	34	+			
Cameroon	51	Lecythidaceae	Oubanguia alata	2639	73.8	34	+	+		
Cameroon	51	Lecythidaceae	Scytopetalum klaineanum	45	76.0	34	+			
Cameroon	51	Phyllanthaceae	Protomegabaria stapfiana	384	58.4	34	+			
Cameroon	51	Phyllanthaceae	Uapaca staudtii	90	69.0	34	(+)			
Cameroon	51	Rubiaceae	Pausinystalia macroceras	49	58.5	34	+			
Cameroon	51	Rutaceae	Zanthoxylum gilletii	120	87.4	34	+			
Cameroon	51	Salicaceae	Homalium longistylum	51	63.2	34	+			
Cameroon	51	Sapotaceae	Lecomtedoxa klaineana	142	185.0	34	(+)	+		
Cameroon	51	Vochysiaceae	Erismadelphus exsul	58	85.0	34	+			
Dem. Rep. Congo	52	Apocynaceae	Alstonia boonei	42	116.3	34	+			
Dem. Rep. Congo	52	Fabaceae	Anthonotha macrophylla	41	60.1	34	(+)			
Dem. Rep. Congo	52	Fabaceae	Cynometra alexandri	1311	123.3	34	+	+		
Dem. Rep. Congo	52	Fabaceae	Erythrophleum suaveolens	101	112.9	34	(-)	+		
Dem. Rep. Congo	52	Fabaceae	Gilbertiodendron dewevrei	3492	142.3	34	+	+	+	
Dem. Rep. Congo	52	Fabaceae	Julbernardia seretii	988	122.3	34	+	+		

Country	Data ref.	Family	Species	# of trees	Max. tree diam. (cm)	Allom. ref.	Bin 1	Bin 2	Bin 3	Bin 4
Dem. Rep. Congo	52	Malvaceae	Cola lateritia	186	67.7	34	+	+		
Dem. Rep. Congo	52	Phyllanthaceae	Cleistanthus michelsonii	197	88.0	34	+	+		
Dem. Rep. Congo	52	Rhizophoraceae	Comiphyton gabonense	44	75.2	34	+			
Dem. Rep. Congo	52	Rubiaceae	Hallea stipulosa	88	84.0	34	(+)	+		
Dem. Rep. Congo	52	Rubiaceae	Sarcocephalus pobeguinii	47	76.8	34	+			
China	53	Betulaceae	Betula platyphylla	90	46.4	54,55	+	+		
China	53	Fagaceae	Quercus mongolica	770	104.2	54,55	+	+		
China	53	Malvaceae	Tilia amurensis	2185	104.4	54,55	+	+		
China	53	Malvaceae	Tilia mandshurica	142	76.5	54,55	(+)			
China	53	Oleaceae	Fraxinus mandshurica	648	100.3	54,55	(+)	+	+	(-)
China	53	Pinaceae	Pinus koraiensis	2387	98.5	54,55	(-)	+	+	(-)
China	53	Rosaceae	Malus baccata	50	48.3	54,55	(+)			
China	53	Sapindaceae	Acer mono	1625	61.0	54,55	(+)	+		
China	53	Ulmaceae	Ulmus japonica	395	100.1	54,55	+	+	+	
Malaysia	56	Anacardiaceae	Gluta laxiflora	458	50.9	34	+			
Malaysia	56	Anacardiaceae	Gluta macrocarpa	168	80.5	34	+	+		
Malaysia	56	Anacardiaceae	Gluta wallichii	72	97.4	34	+	+	(+)	
Malaysia	56	Anacardiaceae	Gluta woodsiana	78	80.2	34	+			
Malaysia	56	Anacardiaceae	Mangifera foetida	81	62.0	34	+			
Malaysia	56	Anacardiaceae	Mangifera parvifolia	293	50.8	34	(+)	+		
Malaysia	56	Anacardiaceae	Swintonia foxworthyi	62	66.5	34	+			
Malaysia	56	Anacardiaceae	Swintonia schwenkii	211	86.1	34	(+)	+		
Malaysia	56	Burseraceae	Canarium pseudopatenti-nervium	54	69.9	34	(+)			
Malaysia	56	Burseraceae	Dacryodes aff. incurvata	161	54.7	34	+			
Malaysia	56	Burseraceae	Dacryodes expansa	507	49.6	34	+			
Malaysia	56	Burseraceae	Dacryodes incurvata	90	64.2	34	+			
Malaysia	56	Burseraceae	Dacryodes rostrata	403	51.6	34	+			
Malaysia	56	Burseraceae	Santiria grandiflora	51	68.0	34	+	+		
Malaysia	56	Burseraceae	Santiria laevigata	263	64.5	34	+	+		
Malaysia	56	Burseraceae	Santiria mollis	81	65.8	34	+			
Malaysia	56	Burseraceae	Santiria rubiginosa	44	89.6	34	+			
Malaysia	56	Burseraceae	Santiria tomentosa	128	62.8	34	(+)	(+)	(+)	(+)
Malaysia	56	Clusiaceae	Calophyllum soulattri	40	95.4	34	(+)	+		
Malaysia	56	Clusiaceae	Garcinia caudiculata	54	58.9	34	+			
Malaysia	56	Clusiaceae	Kayea macrantha	80	46.8	34	+			
Malaysia	56	Crypteroniaceae	Crypteronia macrophylla	105	48.2	34	(+)			
Malaysia	56	Ctenolophonaceae	Ctenolophon parvifolius	74	82.6	34	(+)	+		
Malaysia	56	Dipterocarpaceae	Cotylelobium melanoxylon	48	85.1	34	(+)	+		

Country	Data ref.	Family	Species	# of trees	Max. tree diam. (cm)	Allom. ref.	Bin 1	Bin 2	Bin 3	Bin 4
Malaysia	56	Dipterocarpaceae	Dipterocarpus confertus	47	137.0	34	+	+		
Malaysia	56	Dipterocarpaceae	Dipterocarpus crinitus	51	125.5	34	(+)	+	+	
Malaysia	56	Dipterocarpaceae	Dipterocarpus geniculatus	62	118.2	34	+	+		
Malaysia	56	Dipterocarpaceae	Dipterocarpus globosus	624	118.1	34	+	+		
Malaysia	56	Dipterocarpaceae	Dipterocarpus palembanicus subsp. borneensis	47	116.7	34	+			
Malaysia	56	Dipterocarpaceae	Dipterocarpus palembanicus subsp. palembanicus	43	93.2	34	(-)	+		
Malaysia	56	Dipterocarpaceae	Dryobalanops aromatica	705	144.4	34	+	+		
Malaysia	56	Dipterocarpaceae	Dryobalanops lanceolata	43	123.4	34	+	+		
Malaysia	56	Dipterocarpaceae	Parashorea parvifolia	58	124.5	34	+	+		
Malaysia	56	Dipterocarpaceae	Shorea acuta	361	79.5	34	+	+		
Malaysia	56	Dipterocarpaceae	Shorea amplexicaulis	146	87.4	34	+			
Malaysia	56	Dipterocarpaceae	Shorea beccariana	218	110.2	34	+	+		
Malaysia	56	Dipterocarpaceae	Shorea curtisii	67	136.7	34	+			
Malaysia	56	Dipterocarpaceae	Shorea falciferoides	70	141.4	34	+	+	+	
Malaysia	56	Dipterocarpaceae	Shorea kunstleri	104	127.8	34	(+)	+		
Malaysia	56	Dipterocarpaceae	Shorea laxa	375	114.1	34	+	+		
Malaysia	56	Dipterocarpaceae	Shorea macroptera subsp. baillonii	136	97.3	34	+	+		
Malaysia	56	Dipterocarpaceae	Shorea macroptera subsp. macropterifolia	131	74.0	34	+	+		
Malaysia	56	Dipterocarpaceae	Shorea ovata	57	81.1	34	+			
Malaysia	56	Dipterocarpaceae	Shorea parvifolia	126	126.3	34	+			
Malaysia	56	Dipterocarpaceae	Shorea quadrinervis	110	69.2	34	+			
Malaysia	56	Dipterocarpaceae	Shorea rubella	53	125.7	34	+	+		
Malaysia	56	Dipterocarpaceae	Shorea scaberrima	56	125.5	34	+	+		
Malaysia	56	Dipterocarpaceae	Shorea scrobiculata	76	97.6	34	+	+	(+)	
Malaysia	56	Dipterocarpaceae	Shorea smithiana	129	130.0	34	+	+	+	
Malaysia	56	Dipterocarpaceae	Vatica badiifolia	80	81.1	34	(+)	+		
Malaysia	56	Ebenaceae	Diospyros diepenhorstii	132	58.7	34	+			
Malaysia	56	Euphorbiaceae	Chaetocarpus castanocarpus	174	48.0	34	+			
Malaysia	56	Euphorbiaceae	Elateriospermum tapos	449	51.0	34	+			
Malaysia	56	Fabaceae	Dialium indum	98	72.0	34	+			
Malaysia	56	Fabaceae	Koompassia malaccensis	68	103.0	34	+			
Malaysia	56	Fabaceae	Millettia vasta	44	79.1	34	+			
Malaysia	56	Ixonanthaceae	Allantospermum borneense	714	58.0	34	+	+		
Malaysia	56	Kiggelariaceae	Hydnocarpus pinguis	87	46.6	34	(-)	+		

Country	Data ref.	Family	Species	# of trees	Max. tree diam. (cm)	Allom. ref.	Bin 1	Bin 2	Bin 3	Bin 4
Malaysia	56	Kiggelariaceae	Hydnocarpus woodii	62	71.0	34	+			
Malaysia	56	Lauraceae	Alseodaphne bancana	110	85.0	34	+			
Malaysia	56	Lauraceae	Alseodaphne insignis	115	98.0	34	(-)	(+)	(+)	
Malaysia	56	Malvaceae	Durio acutifolius	71	71.0	34	+			
Malaysia	56	Malvaceae	Durio crassipes	66	104.3	34	+			
Malaysia	56	Malvaceae	Pentace adenophora	82	88.1	34	(+)	+		
Malaysia	56	Moraceae	Artocarpus anisophyllus	116	52.5	34	+			
Malaysia	56	Moraceae	Artocarpus nitidus	89	46.0	34	+			
Malaysia	56	Myristicaceae	Myristica villosa	77	45.8	34	+			
Malaysia	56	Myrtaceae	Cleistocalyx cf. barringtonioides	70	67.2	34	+			
Malaysia	56	Myrtaceae	Syzygium cf. attenuatum	62	65.0	34	+			
Malaysia	56	Myrtaceae	Syzygium cf. grande	221	62.0	34	+			
Malaysia	56	Myrtaceae	Syzygium sp. incert. c	41	75.4	34	(-)	+		
Malaysia	56	Myrtaceae	Whiteodendron moultonianum	576	70.7	34	+			
Malaysia	56	Oxalidaceae	Sarcotheca diversifolia	47	50.9	34	+			
Malaysia	56	Rutaceae	Melicope glabra	58	54.2	34	+			
Malaysia	56	Sapotaceae	Palaquium microphyllum	91	62.7	34	+			
Malaysia	56	Verbenaceae	Teijsmanniodendron simplicifolium	281	60.2	34	+			
Taiwan	57	Anacardiaceae	Rhus succedanea	61	54.0	34	+			
Taiwan	57	Araliaceae	Schefflera octophylla	472	84.1	34	+			
Taiwan	57	Ebenaceae	Diospyros morrisiana	492	60.9	34	+	+		
Taiwan	57	Elaeocarpaceae	Elaeocarpus japonicus	375	72.4	34	(+)	+	+	
Taiwan	57	Fagaceae	Castanopsis cuspidata	1311	99.0	34	+	+	-	
Taiwan	57	Fagaceae	Cyclobalanopsis gilva	118	88.4	34	+			
Taiwan	57	Fagaceae	Cyclobalanopsis longinux	246	52.9	34	+			
Taiwan	57	Fagaceae	Limlia uraiana	1108	171.5	34	(+)	+		
Taiwan	57	Fagaceae	Lithocarpus harlandii	49	59.2	34	+			
Taiwan	57	Juglandaceae	Engelhardia roxburghiana	561	93.3	34	+	+	+	
Taiwan	57	Lauraceae	Cinnamomum micranthum	204	90.6	34	+			
Taiwan	57	Lauraceae	Litsea acuminata	986	67.5	34	+	+	(+)	
Taiwan	57	Lauraceae	Machilus thunbergii	1223	90.0	34	(+)	+		
Taiwan	57	Lauraceae	Machilus zuihoensis	613	79.5	34	+	-		
Taiwan	57	Lythraceae	Lagerstroemia subcostata	83	48.0	34	(+)			
Taiwan	57	Phyllanthaceae	Glochidion acuminatum	394	39.6	34	+			
Taiwan	57	Sabiaceae	Meliosma squamulata	1814	74.8	34	+	+		

Country	Data ref.	Family	Species	# of trees	Max. tree diam. (cm)	Allom. ref.	Bin 1	Bin 2	Bin 3	Bin 4
Taiwan	57	Theaceae	Pyrenaria shinkoensis	1679	43.3	34	+	+	+	
Thailand	58	Anacardiaceae	Gluta obovata	172	90.8	34	+	+		
Thailand	58	Annonaceae	Alphonsea ventricosa	566	71.7	34	+			
Thailand	58	Annonaceae	Polyalthia viridis	2207	46.4	34	+			
Thailand	58	Annonaceae	Saccopetalum lineatum	999	114.6	34	+	+	+	
Thailand	58	Burseraceae	Garuga pinnata	53	87.4	34	+			
Thailand	58	Clusiaceae	Garcinia speciosa	454	68.9	34	+			
Thailand	58	Datiscaceae	Tetrameles nudiflora	205	219.4	34	(+)	+		
Thailand	58	Dipterocarpaceae	Anisoptera costata	75	138.1	34	+	+		
Thailand	58	Dipterocarpaceae	Dipterocarpus alatus	195	149.2	34	(+)	+		
Thailand	58	Dipterocarpaceae	Hopea odorata	182	189.9	34	+	+		
Thailand	58	Dipterocarpaceae	Vatica harmandiana	692	126.8	34	+	+		
Thailand	58	Ebenaceae	Diospyros variegata	381	74.8	34	+	+		
Thailand	58	Ebenaceae	Diospyros winitii	786	45.0	34	+			
Thailand	58	Euphorbiaceae	Macaranga siamensis	90	52.0	34	+			
Thailand	58	Euphorbiaceae	Mallotus philippenensis	121	51.4	34	+			
Thailand	58	Euphorbiaceae	Trewia nudiflora	159	61.7	34	+			
Thailand	58	Irvingiaceae	Irvingia malayana	95	113.0	34	+	+		
Thailand	58	Lamiaceae	Vitex peduncularis	54	71.8	34	+			
Thailand	58	Lauraceae	Neolitsea obtusifolia	500	66.6	34	+	+		
Thailand	58	Lauraceae	Persea sp.	138	63.9	34	+			
Thailand	58	Lythraceae	Lagerstroemia tomentosa	188	137.6	34	+	+		
Thailand	58	Malvaceae	Pterospermum grandiflorum	118	65.1	34	+			
Thailand	58	Meliaceae	Aglaia spectabilis	110	67.2	34	(-)	+	+	
Thailand	58	Meliaceae	Aphanamixis polystachya	71	76.9	34	+			
Thailand	58	Meliaceae	Chukrassia tabularis	96	87.0	34	(+)	+		
Thailand	58	Meliaceae	Dysoxylum grande	72	39.3	34	+			
Thailand	58	Myrtaceae	Syzygium syzgioides	75	68.0	34	+			
Thailand	58	Phyllanthaceae	Baccaurea ramiflora	907	41.4	34	+			
Thailand	58	Polygalaceae	Xanthophyllum flavescens	88	56.7	34	+			
Thailand	58	Sapindaceae	Acer oblongum	175	131.4	34	(+)	+		
Thailand	58	Sapindaceae	Arytera littoralis	818	42.5	34	(-)	+		
Thailand	58	Sapindaceae	Dimocarpus longan	999	92.2	34	+	+		
Thailand	58	Sapindaceae	Harpullia arborea	186	48.6	34	+	-		
New Zealand	59	Cunoniaceae	Weinmannia racemosa	9277	173.8	60	+	+	+	
New Zealand	59	Cupressaceae	Libocedrus bidwillii	56	83.2	60	+			
New Zealand	59	Elaeocarpaceae	Elaeocarpus dentatus	56	85.4	60	+			
New Zealand	59	Elaeocarpaceae	Elaeocarpus hookerianus	91	95.0	60	(-)	+		

Country	Data ref.	Family	Species	# of trees	Max. tree diam. (cm)	Allom. ref.	Bin 1	Bin 2	Bin 3	Bin 4
New Zealand	59	Escalloniaceae	Carpodetus serratus	628	48.3	60	+			
New Zealand	59	Escalloniaceae	Ixerba excelsa	98	58.8	60	+			
New Zealand	59	Escalloniaceae	Quintinia acutifolia	368	39.8	60	+			
New Zealand	59	Fagaceae	Nothofagus fusca	2381	203.5	60	+	+	+	-
New Zealand	59	Fagaceae	Nothofagus menziesii	6855	158.0	60	+	+	+	+
New Zealand	59	Fagaceae	Nothofagus solandri	17595	121.0	60	+	+	+	+
New Zealand	59	Fagaceae	Nothofagus truncata	89	124.5	60	+			
New Zealand	59	Griseliniaceae	Griselinia littoralis	1636	106.3	60	+	+		
New Zealand	59	Lauraceae	Beilschmiedia tawa	304	95.0	60	+			
New Zealand	59	Myrtaceae	Kunzea ericoides	599	78.4	60	(+)	+	+	
New Zealand	59	Myrtaceae	Metrosideros umbellata	1196	267.5	60	+	+		
New Zealand	59	Onagraceae	Fuchsia excorticata	241	66.5	60	+	+		
New Zealand	59	Podocarpaceae	Dacrydium cupressinum	860	193.0	60	+	+	+	
New Zealand	59	Podocarpaceae	Podocarpus hallii	1277	147.7	60	(+)	+		
New Zealand	59	Podocarpaceae	Prumnopitys ferruginea	444	90.5	60	+			
New Zealand	59	Podocarpaceae	Prumnopytis taxifolia	72	65.7	60	+			
New Zealand	59	Proteaceae	Knightia excelsa	175	90.5	60	+	+		
New Zealand	59	Violaceae	Melicytus ramiflorus	1120	138	60	+			
Argentina	61	Anacardiaceae	Astronium urundeuva	212	90.0	34	+	+		
Argentina	61	Betulaceae	Alnus acuminata	145	66.2	34	+			
Argentina	61	Bignoniaceae	Tabebuia impetiginosa	107	62.3	34	+	+		
Argentina	61	Boraginaceae	Cordia trichotoma	100	54.6	34	+			
Argentina	61	Boraginaceae	Patagonula americana	277	77.5	34	+	+		
Argentina	61	Caprifoliaceae	Sambucus nigra	102	50.6	34	(+)			
Argentina	61	Combretaceae	Terminalia triflora	371	85.4	34	+			
Argentina	61	Elaeocarpaceae	Crinodendron tucumanum	175	113.4	34	+	+	(-)	
Argentina	61	Fabaceae	Anadenanthera colubrina	616	127.0	34	+	+		
Argentina	61	Fabaceae	Gleditsia amorphoides	181	45.0	34	+			
Argentina	61	Fabaceae	Myroxylon peruiferum	68	64.0	34	+			
Argentina	61	Fabaceae	Parapiptadenia excelsa	499	89.2	34	(-)	+		
Argentina	61	Fabaceae	Tipuana tipu	46	152.2	34	+	+		
Argentina	61	Juglandaceae	Juglans australis	98	56.7	34	+			
Argentina	61	Lauraceae	Cinnamomum porphyrium	627	174.5	34	+			
Argentina	61	Lauraceae	Ocotea puberula	318	82.5	34	+			
Argentina	61	Malvaceae	Ceiba insigne	78	95.5	34	(+)			

Country	Data ref.	Family	Species	# of trees	Max. tree diam. (cm)	Allom. ref.	Bin 1	Bin 2	Bin 3	Bin 4
Argentina	61	Malvaceae	Heliocarpus popayanensis	56	55.7	34	+			
Argentina	61	Meliaceae	Cedrela balansae	69	100.5	34	+			
Argentina	61	Meliaceae	Cedrela lilloi	75	82.8	34	(-)	+		
Argentina	61	Moraceae	Morus alba	179	76.1	34	(+)	+	(+)	(+)
Argentina	61	Myrtaceae	Blepharocalyx salicifolious	174	132.5	34	(+)	+	+	
Argentina	61	Myrtaceae	Myrcianthes pungens	516	72.6	34	+			
Argentina	61	Nyctaginaceae	Pisonia zapallo	365	84.7	34	+			
Argentina	61	Podocarpaceae	Podocarpus parlatorei	299	151.9	34	+	+		
Argentina	61	Polygonaceae	Ruprechtia laxiflora	93	104.8	34	+	+		
Argentina	61	Primulaceae	Myrsine laetevirens	149	134.4	34	+			
Argentina	61	Rhamnaceae	Phyllostilon rhamnoides	441	88.2	34	+	+		
Argentina	61	Rubiaceae	Callycophylum multiflorum	287	83.7	34	(-)	+		
Argentina	61	Sapindaceae	Cupanea vernalis	128	57.5	34	+			
Argentina	61	Sapindaceae	Diatenopterix sorbifolia	291	54.9	34	(+)	+		
Argentina	61	Sapotaceae	Chrysophyllum gonocarpun	172	75.0	34	+	+		
Colombia	62	Anacardiaceae	Astronium graveolens	290	50.2	63	(+)	+		
Colombia	62	Burseraceae	Bursera simaruba	186	64.9	63	+			
Colombia	62	Dipterocarpaceae	Pseudomonotes tropenbosii	58	72.9	63	+			
Colombia	62	Euphorbiaceae	Croton magdalenensis	52	52.0	63	+			
Colombia	62	Fagaceae	Quercus humboldtii	509	92.5	63	+	+	-	
Colombia	62	Lecythidaceae	Eschweilera punctata	115	69.7	63	+			
Colombia	62	Moraceae	Brosimum utile	115	97.1	63	+			
Panama	64	Anacardiaceae	Spondias radlkoferi	57	93.9	34	(+)	+		
Panama	64	Annonaceae	Guatteria dumetorum	160	67.3	34	(-)	+		
Panama	64	Apocynaceae	Aspidosperma spruceanum	50	111.2	34	+	+		
Panama	64	Apocynaceae	Tabernaemontana arborea	292	82.7	34	+			
Panama	64	Araliaceae	Dendropanax arboreus	64	66.9	34	+	+		
Panama	64	Bignoniaceae	Jacaranda copaia	205	91.6	34	+			
Panama	64	Bignoniaceae	Tabebuia rosea	55	82.5	34	+			
Panama	64	Boraginaceae	Cordia alliodora	49	64.2	34	+			
Panama	64	Boraginaceae	Cordia bicolor	289	45.8	34	+			
Panama	64	Burseraceae	Protium tenuifolium	331	46.3	34	+			
Panama	64	Burseraceae	Tetragastris panamensis	356	74.2	34	+			
Panama	64	Chrysobalanaceae	Hirtella triandra	646	41.0	34	+			
Panama	64	Erythropalaceae	Heisteria concinna	255	38.0	34	+			
Panama	64	Euphorbiaceae	Alchornea costaricensis	87	60.3	34	(+)			
Panama	64	Euphorbiaceae	Hura crepitans	87	246.8	34	(-)	+	+	
Panama	64	Fabaceae	Lonchocarpus heptaphyllus	86	55.7	34	+			
Panama	64	Fabaceae	Prioria copaifera	319	136.9	34	+	+		

Country	Data ref.	Family	Species	# of trees	Max. tree diam. (cm)	Allom. ref.	Bin 1	Bin 2	Bin 3	Bin 4
Panama	64	Fabaceae	Tachigali versicolor	78	63.2	34	(+)	+	+	
Panama	64	Lauraceae	Beilschmiedia pendula	228	79.2	34	+	+		
Panama	64	Lauraceae	Ocotea whitei	97	82.7	34	+			
Panama	64	Lecythidaceae	Gustavia superba	547	44.8	34	+			
Panama	64	Malvaceae	Apeiba membranacea	174	114.3	34	+			
Panama	64	Malvaceae	Luehea seemannii	62	113.9	34	+			
Panama	64	Malvaceae	Quararibea asterolepis	525	92.5	34	+			
Panama	64	Meliaceae	Guarea guidonia	296	44.5	34	+			
Panama	64	Meliaceae	Trichilia tuberculata	1306	64.3	34	+	+		
Panama	64	Moraceae	Brosimum alicastrum	162	129.5	34	(-)	+		
Panama	64	Moraceae	Poulsenia armata	480	80.0	34	+			
Panama	64	Myristicaceae	Virola sebifera	495	42.3	34	+			
Panama	64	Myristicaceae	Virola surinamensis	107	88.5	34	(-)	+		
Panama	64	Nyctaginaceae	Guapira standleyana	78	108.7	34	+			
Panama	64	Putranjivaceae	Drypetes standleyi	276	60.6	34	+	+		
Panama	64	Rubiaceae	Alseis blackiana	881	89.2	34	(+)	+	+	
Panama	64	Rutaceae	Zanthoxylum ekmanii	111	67.4	34	+			
Panama	64	Salicaceae	Casearia arborea	69	54.7	34	+			
Panama	64	Sapotaceae	Pouteria reticulata	169	85.0	34	(+)	+		
Panama	64	Simaroubaceae	Simarouba amara	207	76.7	34	+	+		
Panama	64	Urticaceae	Cecropia insignis	155	56.2	34	+			
Spain	65,66	Aquifoliaceae	Ilex aquifolium	295	51.6	65,66	+			
Spain	65,66	Aquifoliaceae	Ilex canariensis	272	71.6	65,66	+			
Spain	65,66	Betulaceae	Alnus glutinosa	1177	118.4	65,66	+	+	+	
Spain	65,66	Betulaceae	Betula spp.	2343	79.6	65,66	+	+		
Spain	65,66	Cupressaceae	Chamaecyparis lawsoniana	724	50.4	65,66	+	+	+	
Spain	65,66	Cupressaceae	Juniperus communis	684	75.8	65,66	+	+		
Spain	65,66	Cupressaceae	Juniperus thurifera	5900	127.3	65,66	+	+	+	
Spain	65,66	Fagaceae	Castanea sativa	4775	240.6	65,66	(+)	+	+	-
Spain	65,66	Fagaceae	Fagus sylvatica	20676	164.9	65,66	+	+	+	(+)
Spain	65,66	Fagaceae	Quercus ilex	40451	141.6	65,66	+	+	+	-
Spain	65,66	Fagaceae	Quercus petraea	5145	187.8	65,66	(-)	+	+	
Spain	65,66	Fagaceae	Quercus pyrenaica	20466	172.4	65,66	(+)	+	+	(+)
Spain	65,66	Fagaceae	Quercus robur	8866	146.4	65,66	(-)	+	+	-
Spain	65,66	Fagaceae	Quercus suber	10907	146.5	65,66	-	+	+	+
Spain	65,66	Juglandaceae	Juglans regia	68	77.0	65,66	(+)			
Spain	65,66	Lauraceae	Persea indica	201	105.0	65,66	+			
Spain	65,66	Malvaceae	Tilia spp.	97	79.9	65,66	+			
Spain	65,66	Myricaceae	Myrica faya	786	108.2	65,66	+	+	+	
Spain	65,66	Myrtaceae	Eucalyptus camaldulensis	1189	89.1	65,66	-	+	+	+
Spain	65,66	Myrtaceae	Eucalyptus globulus	3465	117.8	65,66	-	+	+	+
Spain	65,66	Myrtaceae	Eucalyptus nitens	189	101.2	65,66	(+)	+		
Spain	65,66	Oleaceae	Olea europaea	389	81.2	65,66	(+)	-	+	
Spain	65,66	Pinaceae	Abies alba	2276	140.1	65,66	(+)	+		
Spain	65,66	Pinaceae	Larix spp.	794	47.9	65,66	(-)	(+)	+	+
Spain	65,66	Pinaceae	Picea abies	94	75.4	65,66	(-)	+		
Spain	65,66	Pinaceae	Pinus canariensis	16044	174.0	65,66	+	+	+	

Country	Data ref.	Family	Species	# of trees	Max. tree diam. (cm)	Allom. ref.	Bin 1	Bin 2	Bin 3	Bin 4
Spain	65,66	Pinaceae	Pinus halepensis	43615	102.8	65,66	(+)	+	+	+
Spain	65,66	Pinaceae	Pinus nigra	44291	95.5	65,66	+	+	+	+
Spain	65,66	Pinaceae	Pinus pinaster	76024	96.4	65,66	+	+	+	+
Spain	65,66	Pinaceae	Pinus pinea	14112	130.5	65,66	+	+	+	-
Spain	65,66	Pinaceae	Pinus radiata	11331	90.7	65,66	(-)	+	+	+
Spain	65,66	Pinaceae	Pinus sylvestris	87225	128.3	65,66	+	+	+	+
Spain	65,66	Pinaceae	Pinus uncinata	10735	127.3	65,66	-	+		
Spain	65,66	Rosaceae	Prunus spp.	223	49.3	65,66	(+)	+		
Spain	65,66	Rosaceae	Sorbus spp.	327	65.3	65,66	(-)	(+)		
Spain	65,66	Salicaceae	Populus alba	209	91.7	65,66	(-)	+		
Spain	65,66	Salicaceae	Populus nigra	1189	101.9	65,66	(-)	+		
Spain	65,66	Salicaceae	Populus tremula	454	90.5	65,66	+			
Spain	65,66	Salicaceae	Salix spp.	636	105.0	65,66	(-)	+	(+)	
Spain	65,66	Sapindaceae	Acer campestre	1091	89.1	65,66	(+)	+		
Spain	65,66	Taxaceae	Taxus baccata	40	107.6	65,66	(-)	+		
Spain	65,66	Ulmaceae	Ulmus minor	114	111.4	65,66	+			
United States (east)	67	Betulaceae	Betula alleghaniensis	1245	102.4	17	(+)	+		
United States (east)	67	Betulaceae	Betula lenta	244	60.2	17	+			
United States (east)	67	Betulaceae	Betula nigra	212	81.0	17	+	+		
United States (east)	67	Betulaceae	Betula papyrifera	1506	63.0	17	+	+	+	
United States (east)	67	Cornaceae	Nyssa aquatica	53	101.1	17	-			
United States (east)	67	Cornaceae	Nyssa sylvatica	682	75.7	17	+			
United States (east)	67	Cupressaceae	Juniperus virginiana	800	60.7	17	(-)	+		
United States (east)	67	Cupressaceae	Thuja occidentalis	4337	80.8	17	+	+		
United States (east)	67	Fabaceae	Gleditsia triacanthos	304	103.9	17	+	+		
United States (east)	67	Fabaceae	Robinia psuedoacacia	443	64.8	17	+	+		
United States (east)	67	Fagaceae	Fagus grandifolia	2130	109.5	17	+	+	+	
United States (east)	67	Fagaceae	Quercus alba	6583	127.8	17	(+)	+	+	+
United States (east)	67	Fagaceae	Quercus bicolor	210	100.6	17	+	+		
United States (east)	67	Fagaceae	Quercus coccinea	878	68.1	17	-	+	+	+
United States (east)	67	Fagaceae	Quercus ellipsoidalis	226	76.7	17	+	+	+	

Country	Data ref.	Family	Species	# of trees	Max. tree diam. (cm)	Allom. ref.	Bin 1	Bin 2	Bin 3	Bin 4
United States (east)	67	Fagaceae	Quercus falcata var. falcata	249	100.1	17	+	+		
United States (east)	67	Fagaceae	Quercus falcata var. pagodaefolia	60	80.8	17	(-)	+		
United States (east)	67	Fagaceae	Quercus imbricaria	310	72.1	17	-	+	+	
United States (east)	67	Fagaceae	Quercus macrocarpa	224	116.8	17	+	+		
United States (east)	67	Fagaceae	Quercus michauxii	45	107.7	17	+	+		
United States (east)	67	Fagaceae	Quercus muehlenbergii	439	94.5	17	(+)	+	+	+
United States (east)	67	Fagaceae	Quercus palustris	584	138.7	17	(+)	+	+	
United States (east)	67	Fagaceae	Quercus prinus	1900	93.7	17	+	+	+	+
United States (east)	67	Fagaceae	Quercus rubra	4477	157.7	17	+	+	+	
United States (east)	67	Fagaceae	Quercus shumardii	62	104.9	17	+			
United States (east)	67	Fagaceae	Quercus stellata	711	74.4	17	+	+	+	
United States (east)	67	Fagaceae	Quercus velutina	3867	104.4	17	+	+	+	+
United States (east)	67	Hamamelidaceae	Liquidambar styraciflua	777	72.6	17	(+)	+		
United States (east)	67	Juglandaceae	Carya cordiformis	774	81.0	17	+	+		
United States (east)	67	Juglandaceae	Carya glabra	2060	95.8	17	(+)	+	+	
United States (east)	67	Juglandaceae	Carya laciniosa	74	68.3	17	+			
United States (east)	67	Juglandaceae	Carya ovata	1602	82.6	17	(-)	+	+	
United States (east)	67	Juglandaceae	Carya tomentosa	975	93.5	17	+	+		
United States (east)	67	Juglandaceae	Juglans nigra	1108	82.6	17	-	+	+	+
United States (east)	67	Lauraceae	Sassafras albidum	895	75.7	17	+	+	+	(+)
United States (east)	67	Magnoliaceae	Liriodendron tulipifera	3239	117.1	17	-	+	+	+

Country	Data ref.	Family	Species	# of trees	Max. tree diam. (cm)	Allom. ref.	Bin 1	Bin 2	Bin 3	Bin 4
United States (east)	67	Magnoliaceae	Magnolia acuminata	98	55.1	17	+			
United States (east)	67	Malvaceae	Tilia americana	1571	122.7	17	+	+	+	
United States (east)	67	Moraceae	Maclura pomifera	174	61.7	17	+	+		
United States (east)	67	Oleaceae	Fraxinus americana	2354	137.2	17	-	+	+	+
United States (east)	67	Oleaceae	Fraxinus nigra	712	58.2	17	+	+		
United States (east)	67	Oleaceae	Fraxinus pennsylvanica	906	115.6	17	+	+		
United States (east)	67	Pinaceae	Abies balsamea	1227	40.1	17	+			
United States (east)	67	Pinaceae	Larix laricina	646	57.2	17	+	+		
United States (east)	67	Pinaceae	Picea glauca	759	73.9	17	(+)	+		
United States (east)	67	Pinaceae	Picea mariana	1124	49.8	17	+	+		
United States (east)	67	Pinaceae	Picea rubens	412	46.5	17	+			
United States (east)	67	Pinaceae	Pinus banksiana	1245	47.5	17	+	+		
United States (east)	67	Pinaceae	Pinus echinata	596	71.4	17	(-)	+		
United States (east)	67	Pinaceae	Pinus resinosa	2173	65.5	17	(-)	+	+	+
United States (east)	67	Pinaceae	Pinus rigida	299	46.2	17	+	+		
United States (east)	67	Pinaceae	Pinus strobus	2728	108.0	17	+	+		
United States (east)	67	Pinaceae	Pinus taeda	597	58.2	17	(+)	+		
United States (east)	67	Pinaceae	Pinus virginiana	921	55.4	17	+	+		
United States (east)	67	Pinaceae	Tsuga canadensis	2071	100.1	17	+	+	+	
United States (east)	67	Platanaceae	Platanus occidentalis	1073	133.9	17	-	+	+	
United States (east)	67	Rosaceae	Prunus serotina	1532	88.9	17	+	+	+	

Country	Data ref.	Family	Species	# of trees	Max. tree diam. (cm)	Allom. ref.	Bin 1	Bin 2	Bin 3	Bin 4
United States (east)	67	Salicaceae	Populus balsamifera	381	82.8	17	+	+	+	
United States (east)	67	Salicaceae	Populus deltoides	648	147.1	17	-	+		
United States (east)	67	Salicaceae	Populus grandidentata	1242	66.5	17	+	+		
United States (east)	67	Salicaceae	Populus tremuloides	2270	62.5	17	+	+	+	
United States (east)	67	Salicaceae	Salix nigra	164	88.4	17	+			
United States (east)	67	Sapindaceae	Acer negundo	417	100.8	17	+	+		
United States (east)	67	Sapindaceae	Acer rubrum	7448	124.0	17	+	+	+	+
United States (east)	67	Sapindaceae	Acer saccharinum	1386	121.2	17	(+)	+	+	+
United States (east)	67	Sapindaceae	Acer saccharum	8681	113.3	17	+	+	+	
United States (east)	67	Sapindaceae	Aesculus glabra	85	61.7	17	(+)	+		
United States (east)	67	Ulmaceae	Celtis occidentalis	552	130.6	17	(+)	+	+	(+)
United States (east)	67	Ulmaceae	Ulmus americana	884	72.4	17	+	+		
United States (east)	67	Ulmaceae	Ulmus rubra	415	72.9	17	(+)	+	+	
United States (west)	68,69	Cupressaceae	Calocedrus decurrens	1587	176.0	17	(+)	+	+	+
United States (west)	68,69	Cupressaceae	Chamaecyparis nootkatensis	572	210.0	17	+	+	+	
United States (west)	68,69	Cupressaceae	Thuja plicata	284	240.7	17	+	+		
United States (west)	68,69	Fagaceae	Quercus kelloggii	422	97.8	17	(+)	+		
United States (west)	68,69	Pinaceae	Abies amabilis	2595	124.7	17	+	+	+	(+)
United States (west)	68,69	Pinaceae	Abies concolor	3248	166.8	17	+	+	+	
United States (west)	68,69	Pinaceae	Abies magnifica	1644	249.7	17	+	+	+	+
United States (west)	68,69	Pinaceae	Abies procera	205	230.2	17	+	+		

Country	Data ref.	Family	Species	# of trees	Max. tree diam. (cm)	Allom. ref.	Bin 1	Bin 2	Bin 3	Bin 4
United States (west)	68,69	Pinaceae	Picea sitchensis	409	270.5	17	+	+	(+)	+
United States (west)	68,69	Pinaceae	Pinus albicaulis	550	41.8	17	+			
United States (west)	68,69	Pinaceae	Pinus balfouriana	152	153.0	17	(+)			
United States (west)	68,69	Pinaceae	Pinus contorta	155	70.0	17	(+)	+		
United States (west)	68,69	Pinaceae	Pinus jeffreyi	99	136.6	17	+			
United States (west)	68,69	Pinaceae	Pinus lambertiana	564	196.9	17	+	+	+	+
United States (west)	68,69	Pinaceae	Pinus monticola	215	234.2	17	+	+	+	
United States (west)	68,69	Pinaceae	Pinus ponderosa	2191	175.5	17	+	+	+	
United States (west)	68,69	Pinaceae	Pseudotsuga menziesii	744	225.6	17	(+)	+	+	+
United States (west)	68,69	Pinaceae	Tsuga heterophylla	2253	190.8	17	+	+	+	+
United States (west)	68,69	Pinaceae	Tsuga mertensiana	188	115.1	17	(+)	+		

Data ref. = publication(s) describing our data source for each species; **Allom. ref.** = publication(s) from which we obtained allometric equations for each species. A "+" or "-" symbol in a numbered **Bin** column indicates that the model receiving the greatest weight of evidence by AIC included that bin (line segment); for example, a species having a symbol under **Bin 1** and **Bin 2** but not under **Bin 3** and **Bin 4** was fit with two line segments. "+" indicates that the line segment had a positive slope (mass growth rate increased with tree size within the bin); "-" indicates a negative slope. Symbols without parentheses indicate that the slope for that bin for that particular species was significant at $P \leq 0.05$.

51. Chuyong, G. B. *et al.* in *Tropical Forest Diversity and Dynamism: Findings from a Large-Scale Plot Network* (eds Losos, E. C. & Leigh, E. G. Jr.) 506–516 (University of Chicago Press, 2004).

52. Makana, J.-R. *et al.* in *Tropical Forest Diversity and Dynamism: Findings from a Large-Scale Plot Network* (eds Losos, E. C. & Leigh, E. G. Jr.) 492–505 (University of Chicago Press, 2004).

53. Wang, X. *et al.* Spatial distributions of species in an old-growth temperate forest, northeastern China. *Can. J. For. Res.* **40**, 1011–1019 (2010).

54. Xu, Z., Li, X. & Dai, H. Study on biomass of species in broad-leaved Korean pine mixed forest in Changbai Mountain [in Chinese]. *Forest Ecosyst. Res.* **5**, 33–46 (1985).

55. Wang, C. Biomass allometric equations for 10 co-occurring tree species in Chinese temperate forests. *For. Ecol. Manage.* **222**, 9–16 (2006).

56. Lee, H. S. *et al.* in *Tropical Forest Diversity and Dynamism: Findings from a Large-Scale Plot Network* (eds Losos, E. C. & Leigh, E. G. Jr.) 527-539 (University of Chicago Press, 2004).

57. Su, S. H. *et al. Fushan Subtropical Forest Dynamics Plot: Tree Species Characteristics and Distribution Patterns*. (Taiwan Forestry Research Institute: Taipei, Taiwan, 2007).

58. Bunyavejchewin, S., Baker, P. J., LaFrankie, J. V. & Ashton, P. S. in *Tropical Forest Diversity and Dynamism: Findings from a Large-Scale Plot Network* (eds Losos, E. C. & Leigh, E. G. Jr.) 482-491 (University of Chicago Press, 2004).

59. Wiser, S. K., Bellingham, P. J. & Burrows, L. E. Managing biodiversity information: development of New Zealand's National Vegetation Survey databank. *New Zealand J. Ecol.* **25**, 1–17 (2001).

60. Coomes, D. A., Allen, R. B., Scott, N. A., Goulding, C. & Beets, P. Designing systems to monitor carbon stocks in forests and shrublands. *For. Ecol. Manage.* **164**, 89–108 (2002).

61. Easdale, T. A., Healey, J. R., Grau, H. R. & Malizia, A. Tree life histories in a montane subtropical forest: species differ independently by shade-tolerance, turnover rate and substrate preference. *J. Ecol.* **95**, 1234–1249 (2007).

62. Phillips Bernal, J. F. *et al. Estimación de las Reservas Potenciales de Carbono Almacenadas en la Biomasa Aérea en Bosques Naturales de Colombia*. (Instituto de Hidrología, Meteorología, y Estudios Ambientales: Bogotá D.C., Colombia, 2011).

63. Alvarez, E. *et al.* Tree above-ground biomass allometries for carbon stocks estimation in the natural forests of Colombia. *For. Ecol. Manage.* **267**, 297–308 (2012).

64. Leigh, E. G. Jr. *et al.* in *Tropical Forest Diversity and Dynamism: Findings from a Large-Scale Plot Network* (eds Losos, E. C. & Leigh, E. G. Jr.) 451-463 (University of Chicago Press, 2004).

65. Ministerio de Medio Ambiente (IFN2: MMA) *Segundo Inventario Forestal Nacional (1986–1996): Bases de Datos e Información Cartográfica*. (Banco de Datos de la Naturaleza, Ministerio de Medio Ambiente: Madrid, Spain, 1996).

66. Ministerio de Medio Ambiente (IFN3: MMA) *Tercer Inventario Forestal Nacional (1997-2007): Bases de Datos e Información Cartográfica*. (Banco de Datos de la Naturaleza, Ministerio de Medio Ambiente: Madrid, Spain, 2007).

67. Canham, C. D. & Thomas, R. Q. Frequency, not relative abundance, of temperate tree species varies along climate gradients in eastern North America. *Ecology* **91**, 3433–3440 (2010).

68. Acker, S. A., McKee, W. A., Harmon, M. E. & Franklin, J. F. in *Forest Biodiversity in North, Central and South America, and the Caribbean: Research and Monitoring* (eds Dallmeier, J. & Comisky, A.) 93–106 (Man and the Biosphere Series, Vol. 21, UNESCO and Parthenon Publishing Group: Paris & New York, 1998).

69. Stephenson, N. L. & van Mantgem, P. J. Forest turnover rates follow global and regional patterns of productivity. *Ecol. Lett.* **8**, 524–531 (2005).

LETTER

doi:10.1038/nature12914

Rate of tree carbon accumulation increases continuously with tree size

N. L. Stephenson[1], A. J. Das[1], R. Condit[2], S. E. Russo[3], P. J. Baker[4], N. G. Beckman[3]†, D. A. Coomes[5], E. R. Lines[6], W. K. Morris[7], N. Rüger[2,8]†, E. Álvarez[9], C. Blundo[10], S. Bunyavejchewin[11], G. Chuyong[12], S. J. Davies[13], Á. Duque[14], C. N. Ewango[15], O. Flores[16], J. F. Franklin[17], H. R. Grau[10], Z. Hao[18], M. E. Harmon[19], S. P. Hubbell[2,20], D. Kenfack[13], Y. Lin[21], J.-R. Makana[15], A. Malizia[10], L. R. Malizia[22], R. J. Pabst[19], N. Pongpattananurak[23], S.-H. Su[24], I-F. Sun[25], S. Tan[26], D. Thomas[27], P. J. van Mantgem[28], X. Wang[18], S. K. Wiser[29] & M. A. Zavala[30]

Forests are major components of the global carbon cycle, providing substantial feedback to atmospheric greenhouse gas concentrations[1]. Our ability to understand and predict changes in the forest carbon cycle—particularly net primary productivity and carbon storage—increasingly relies on models that represent biological processes across several scales of biological organization, from tree leaves to forest stands[2,3]. Yet, despite advances in our understanding of productivity at the scales of leaves and stands, no consensus exists about the nature of productivity at the scale of the individual tree[4–7], in part because we lack a broad empirical assessment of whether rates of absolute tree mass growth (and thus carbon accumulation) decrease, remain constant, or increase as trees increase in size and age. Here we present a global analysis of 403 tropical and temperate tree species, showing that for most species mass growth rate increases continuously with tree size. Thus, large, old trees do not act simply as senescent carbon reservoirs but actively fix large amounts of carbon compared to smaller trees; at the extreme, a single big tree can add the same amount of carbon to the forest within a year as is contained in an entire mid-sized tree. The apparent paradoxes of individual tree growth increasing with tree size despite declining leaf-level[8–10] and stand-level[10] productivity can be explained, respectively, by increases in a tree's total leaf area that outpace declines in productivity per unit of leaf area and, among other factors, age-related reductions in population density. Our results resolve conflicting assumptions about the nature of tree growth, inform efforts to understand and model forest carbon dynamics, and have additional implications for theories of resource allocation[11] and plant senescence[12].

A widely held assumption is that after an initial period of increasing growth, the mass growth rate of individual trees declines with increasing tree size[4,5,13–16]. Although the results of a few single-species studies have been consistent with this assumption[15], the bulk of evidence cited in support of declining growth is not based on measurements of individual tree mass growth. Instead, much of the cited evidence documents either the well-known age-related decline in net primary productivity (hereafter 'productivity') of even-aged forest stands[10] (in which the trees are all of a similar age) or size-related declines in the rate of mass gain per unit leaf area (or unit leaf mass)[8–10], with the implicit assumption that declines at these scales must also apply at the scale of the individual tree. Declining tree growth is also sometimes inferred from life-history theory to be a necessary corollary of increasing resource allocation to reproduction[11,16]. On the other hand, metabolic scaling theory predicts that mass growth rate should increase continuously with tree size[6], and this prediction has also received empirical support from a few site-specific studies[6,7]. Thus, we are confronted with two conflicting generalizations about the fundamental nature of tree growth, but lack a global assessment that would allow us to distinguish clearly between them.

To fill this gap, we conducted a global analysis in which we directly estimated mass growth rates from repeated measurements of 673,046 trees belonging to 403 tropical, subtropical and temperate tree species, spanning every forested continent. Tree growth rate was modelled as a function of log(tree mass) using piecewise regression, where the independent variable was divided into one to four bins. Conjoined line segments were fitted across the bins (Fig. 1).

For all continents, aboveground tree mass growth rates (and, hence, rates of carbon gain) for most species increased continuously with tree mass (size) (Fig. 2). The rate of mass gain increased with tree mass in each model bin for 87% of species, and increased in the bin that included the largest trees for 97% of species; the majority of increases were statistically significant (Table 1, Extended Data Fig. 1 and Supplementary Table 1). Even when we restricted our analysis to species achieving the largest sizes (maximum trunk diameter >100 cm; 33% of species), 94% had increasing mass growth rates in the bin that included the largest trees. We found no clear taxonomic or geographic patterns among the 3% of species with declining growth rates in their largest trees, although the small number of these species (thirteen) hampers inference. Declining species included both angiosperms and gymnosperms in seven of the 76 families in our study; most of the seven families had only one or two declining species and no family was dominated by declining species (Supplementary Table 1).

When we log-transformed mass growth rate in addition to tree mass, the resulting model fits were generally linear, as predicted by metabolic scaling theory[6] (Extended Data Fig. 2). Similar to the results of our main

[1]US Geological Survey, Western Ecological Research Center, Three Rivers, California 93271, USA. [2]Smithsonian Tropical Research Institute, Apartado 0843-03092, Balboa, Republic of Panama. [3]School of Biological Sciences, University of Nebraska, Lincoln, Nebraska 68588, USA. [4]Department of Forest and Ecosystem Science, University of Melbourne, Victoria 3121, Australia. [5]Department of Plant Sciences, University of Cambridge, Cambridge CB2 3EA, UK. [6]Department of Geography, University College London, London WC1E 6BT, UK. [7]School of Botany, University of Melbourne, Victoria 3010, Australia. [8]Spezielle Botanik und Funktionelle Biodiversität, Universität Leipzig, 04103 Leipzig, Germany. [9]Jardín Botánico de Medellín, Calle 73, No. 51D-14, Medellín, Colombia. [10]Instituto de Ecología Regional, Universidad Nacional de Tucumán, 4107 Yerba Buena, Tucumán, Argentina. [11]Research Office, Department of National Parks, Wildlife and Plant Conservation, Bangkok 10900, Thailand. [12]Department of Botany and Plant Physiology, Buea, Southwest Province, Cameroon. [13]Smithsonian Institution Global Earth Observatory—Center for Tropical Forest Science, Smithsonian Institution, PO Box 37012, Washington, DC 20013, USA. [14]Universidad Nacional de Colombia, Departamento de Ciencias Forestales, Medellín, Colombia. [15]Wildlife Conservation Society, Kinshasa/Gombe, Democratic Republic of the Congo. [16]Unité Mixte de Recherche—Peuplements Végétaux et Bioagresseurs en Milieu Tropical, Université de la Réunion/CIRAD, 97410 Saint Pierre, France. [17]School of Environmental and Forest Sciences, University of Washington, Seattle, Washington 98195, USA. [18]State Key Laboratory of Forest and Soil Ecology, Institute of Applied Ecology, Chinese Academy of Sciences, Shenyang 110164, China. [19]Department of Forest Ecosystems and Society, Oregon State University, Corvallis, Oregon 97331, USA. [20]Department of Ecology and Evolutionary Biology, University of California, Los Angeles, California 90095, USA. [21]Department of Life Science, Tunghai University, Taichung City 40704, Taiwan. [22]Facultad de Ciencias Agrarias, Universidad Nacional de Jujuy, 4600 San Salvador de Jujuy, Argentina. [23]Faculty of Forestry, Kasetsart University, ChatuChak Bangkok 10900, Thailand. [24]Taiwan Forestry Research Institute, Taipei 10066, Taiwan. [25]Department of Natural Resources and Environmental Studies, National Dong Hwa University, Hualien 97401, Taiwan. [26]Sarawak Forestry Department, Kuching, Sarawak 93660, Malaysia. [27]Department of Botany and Plant Pathology, Oregon State University, Corvallis, Oregon 97331, USA. [28]US Geological Survey, Western Ecological Research Center, Arcata, California 95521, USA. [29]Landcare Research, PO Box 40, Lincoln 7640, New Zealand. [30]Forest Ecology and Restoration Group, Department of Life Sciences, University of Alcalá, Alcalá de Henares, 28805 Madrid, Spain. †Present addresses: Mathematical Biosciences Institute, Ohio State University, Columbus, Ohio 43210, USA (N.G.B.); German Centre for Integrative Biodiversity Research (iDiv), Halle-Jena-Leipzig, 04103 Leipzig, Germany (N.R.).

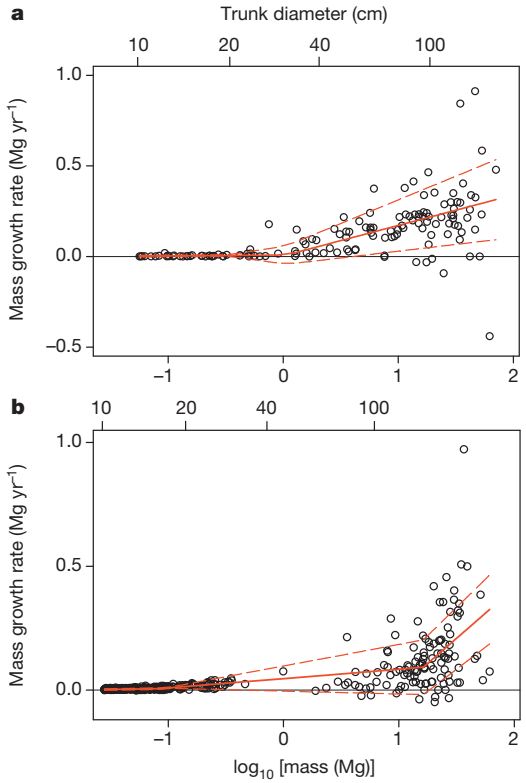

Figure 1 | Example model fits for tree mass growth rates. The species shown are the angiosperm species (*Lecomtedoxa klaineana*, Cameroon, 142 trees) (**a**) and gymnosperm species (*Picea sitchensis*, USA, 409 trees) (**b**) in our data set that had the most massive trees (defined as those with the greatest cumulative aboveground dry mass in their five most massive trees). Each point represents a single tree; the solid red lines represent best fits selected by our model; and the dashed red lines indicate one standard deviation around the predicted values.

analysis using untransformed growth, of the 381 log-transformed species analysed (see Methods), the log-transformed growth rate increased in the bin containing the largest trees for 96% of species.

In absolute terms, trees 100 cm in trunk diameter typically add from 10 kg to 200 kg of aboveground dry mass each year (depending on species), averaging 103 kg per year. This is nearly three times the rate for trees of the same species at 50 cm in diameter, and is the mass equivalent to adding an entirely new tree of 10–20 cm in diameter to the forest each year. Our findings further indicate that the extraordinary growth recently reported in an intensive study of large *Eucalyptus regnans* and *Sequoia sempervirens*[7], which included some of the world's most massive individual trees, is not a phenomenon limited to a few unusual species. Rather, rapid growth in giant trees is the global norm, and can exceed 600 kg per year in the largest individuals (Fig. 3).

Our data set included many natural and unmanaged forests in which the growth of smaller trees was probably reduced by asymmetric competition with larger trees. To explore the effects of competition, we calculated mass growth rates for 41 North American and European species that had published equations for diameter growth rate in the absence of competition. We found that, even in the absence of competition, 85% of the species had mass growth rates that increased continuously with tree size (Extended Data Fig. 3), with growth curves closely resembling those in Fig. 2. Thus, our finding of increasing growth not only has broad generality across species, continents and forest biomes (tropical, subtropical and temperate), it appears to hold regardless of competitive environment.

Importantly, our finding of continuously increasing growth is compatible with the two classes of observations most often cited as evidence of declining, rather than increasing, individual tree growth: with increasing tree size and age, productivity usually declines at the scales of both tree organs (leaves) and tree populations (even-aged forest stands).

First, although growth efficiency (tree mass growth per unit leaf area or leaf mass) often declines with increasing tree size[8–10], empirical observations and metabolic scaling theory both indicate that, on average, total tree leaf mass increases as the square of trunk diameter[17,18]. A typical tree that experiences a tenfold increase in diameter will therefore undergo a roughly 100-fold increase in total leaf mass and a 50–100-fold

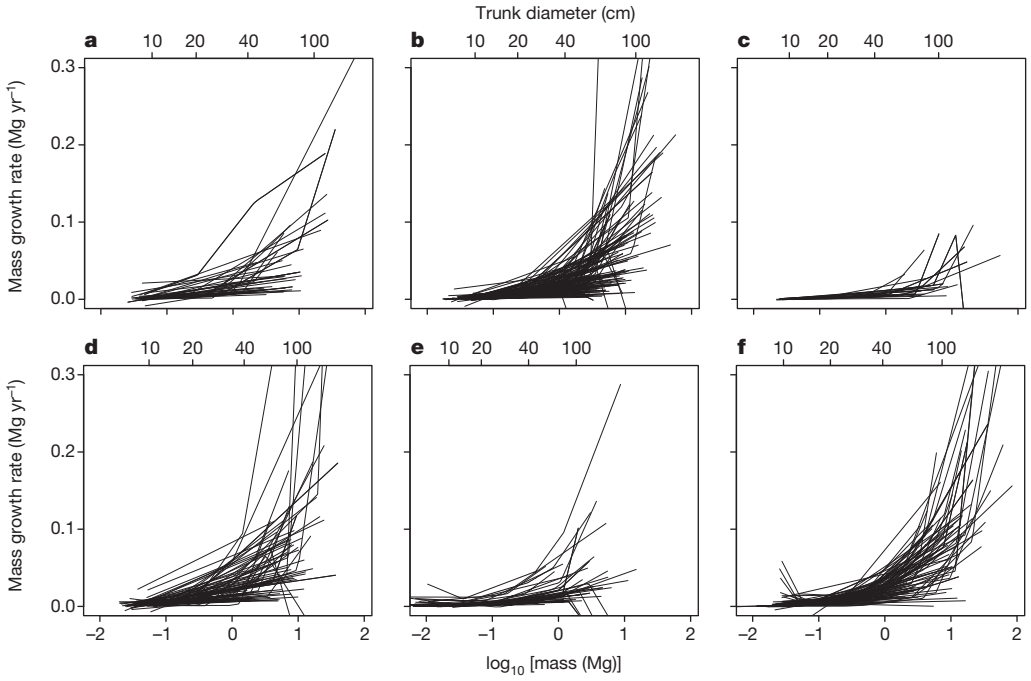

Figure 2 | Aboveground mass growth rates for the 403 tree species, by continent. **a**, Africa (Cameroon, Democratic Republic of the Congo); **b**, Asia (China, Malaysia, Taiwan, Thailand); **c**, Australasia (New Zealand); **d**, Central and South America (Argentina, Colombia, Panama); **e**, Europe (Spain); and **f**, North America (USA). Numbers of trees, numbers of species and percentages with increasing growth are given in Table 1. Trunk diameters are approximate values for reference, based on the average diameters of trees of a given mass.

Table 1 | Sample sizes and tree growth trends by continent

Continent	Number of trees	Number of species	Percentage of species with increasing mass growth rate in the largest trees (percentage significant at $P \leq 0.05$)
Africa	15,366	37	100.0 (86.5)
Asia	43,690	136	96.3 (89.0)
Australasia	45,418	22	95.5 (95.5)
Central and South America	18,530	77	97.4 (92.2)
Europe	439,889	42	90.5 (78.6)
North America	110,153	89	98.9 (94.4)
Total	673,046	403	96.8 (89.8)

The largest trees are those in the last bin fitted by the model. Countries are listed in the legend for Fig. 2.

increase in total leaf area (depending on size-related increases in leaf mass per unit leaf area[19,20]). Parallel changes in growth efficiency can range from a modest increase (such as in stands where small trees are suppressed by large trees)[21] to as much as a tenfold decline[22], with most changes falling in between[8,9,19,22]. At one extreme, the net effect of a low (50-fold) increase in leaf area combined with a large (tenfold) decline in growth efficiency would still yield a fivefold increase in individual tree mass growth rate; the opposite extreme would yield roughly a 100-fold increase. Our calculated 52-fold greater average mass growth rate of trees 100 cm in diameter compared to those 10 cm in diameter falls within this range. Thus, although growth efficiency often declines with increasing tree size, increases in a tree's total leaf area are sufficient to overcome this decline and cause whole-tree carbon accumulation rate to increase.

Second, our findings are similarly compatible with the well-known age-related decline in productivity at the scale of even-aged forest stands. Although a review of mechanisms is beyond the scope of this paper[10,23], several factors (including the interplay of changing growth efficiency and tree dominance hierarchies[24]) can contribute to declining productivity at the stand scale. We highlight the fact that increasing individual tree growth rate does not automatically result in increasing stand productivity because tree mortality can drive orders-of-magnitude reductions in population density[25,26]. That is, even though the large trees in older, even-aged stands may be growing more rapidly, such stands have fewer trees. Tree population dynamics, especially mortality, can thus be a significant contributor to declining productivity at the scale of the forest stand[23].

For a large majority of species, our findings support metabolic scaling theory's qualitative prediction of continuously increasing growth at the scale of individual trees[6], with several implications. For example, life-history theory often assumes that tradeoffs between plant growth and reproduction are substantial[11]. Contrary to some expectations[11,16], our results indicate that for most tree species size-related changes in reproductive allocation are insufficient to drive long-term declines in growth rates[6]. Additionally, declining growth is sometimes considered to be a defining feature of plant senescence[12]. Our findings are thus relevant to understanding the nature and prevalence of senescence in the life history of perennial plants[27].

Finally, our results are relevant to understanding and predicting forest feedbacks to the terrestrial carbon cycle and global climate system[1–3]. These feedbacks will be influenced by the effects of climatic, land-use and other environmental changes on the size-specific growth rates and size structure of tree populations—effects that are already being observed in forests[28,29]. The rapid growth of large trees indicates that, relative to their numbers, they could play a disproportionately important role in these feedbacks[30]. For example, in our western USA old-growth forest plots, trees >100 cm in diameter comprised 6% of trees, yet contributed 33% of the annual forest mass growth. Mechanistic models of the forest carbon cycle will depend on accurate representation of productivity across several scales of biological organization, including calibration and validation against continuously increasing carbon accumulation rates at the scale of individual trees.

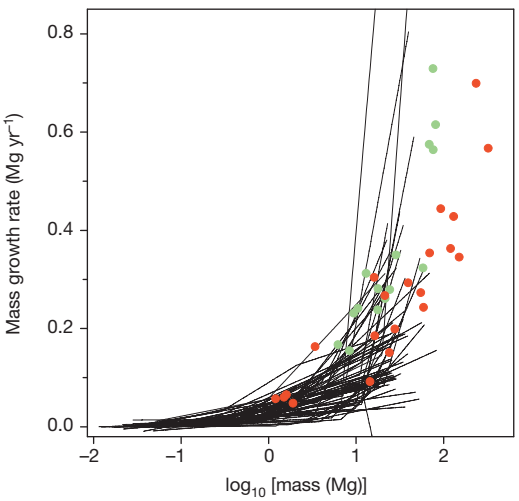

Figure 3 | Aboveground mass growth rates of species in our data set compared with *E. regnans* and *S. sempervirens*. For clarity, only the 58 species in our data set having at least one tree exceeding 20 Mg are shown (lines). Data for *E. regnans* (green dots, 15 trees) and *S. sempervirens* (red dots, 21 trees) are from an intensive study that included some of the most massive individual trees on Earth[7]. Both axes are expanded relative to those of Fig. 2.

METHODS SUMMARY

We estimated aboveground dry mass growth rates from consecutive diameter measurements of tree trunks—typically measured every five to ten years—from long-term monitoring plots. Analyses were restricted to trees with trunk diameter ≥10 cm, and to species having ≥40 trees in total and ≥15 trees with trunk diameter ≥30 cm. Maximum trunk diameters ranged from 38 cm to 270 cm among species, averaging 92 cm. We converted each diameter measurement (plus an accompanying height measurement for 16% of species) to aboveground dry mass, M, using published allometric equations. We estimated tree growth rate as $G = \Delta M/\Delta t$ and modelled G as a function of $\log(M)$ for each species using piecewise regression. The independent variable $\log(M)$ was divided into bins and a separate line segment was fitted to G versus $\log(M)$ in each bin so that the line segments met at the bin divisions. Bin divisions were not assigned a priori, but were fitted by the model separately for each species. We fitted models with 1, 2, 3 and 4 bins, and selected the model receiving the most support by Akaike's Information Criterion for each species. Our approach thus makes no assumptions about the shape of the relationship between G and $\log(M)$, and can accommodate increasing, decreasing or hump-shaped relationships. Parameters were fitted with a Gibbs sampler based on Metropolis updates, producing credible intervals for model parameters and growth rates at any diameter; uninformative priors were used for all parameters. We tested extensively for bias, and found no evidence that our results were influenced by model fits failing to detect a final growth decline in the largest trees, possible biases introduced by the 47% of species for which we combined data from several plots, or possible biases introduced by allometric equations (Extended Data Figs 4 and 5).

Online Content Any additional Methods, Extended Data display items and Source Data are available in the online version of the paper; references unique to these sections appear only in the online paper.

Received 5 August; accepted 27 November 2013.
Published online 15 January 2014.

1. Pan, Y. *et al.* A large and persistent carbon sink in the world's forests. *Science* **333,** 988–993 (2011).

2. Medvigy, D., Wofsy, S. C., Munger, J. W., Hollinger, D. Y. & Moorcroft, P. R. Mechanistic scaling of ecosystem function and dynamics in space and time: Ecosystem Demography model version 2. *J. Geophys. Res.* **114,** G01002 (2009).
3. Caspersen, J. P., Vanderwel, M. C., Cole, W. G. & Purves, D. W. How stand productivity results from size- and competition-dependent growth and mortality. *PLoS ONE* **6,** e28660 (2011).
4. Kutsch, W. L. *et al.* in *Old-Growth Forests: Function, Fate and Value* (eds Wirth, C., Gleixner, G. & Heimann, M.) 57–79 (Springer, 2009).
5. Meinzer, F. C., Lachenbruch, B. & Dawson, T. E. (eds) *Size- and Age-Related Changes in Tree Structure and Function* (Springer, 2011).
6. Enquist, B. J., West, G. B., Charnov, E. L. & Brown, J. H. Allometric scaling of production and life-history variation in vascular plants. *Nature* **401,** 907–911 (1999).
7. Sillett, S. C. *et al.* Increasing wood production through old age in tall trees. *For. Ecol. Manage.* **259,** 976–994 (2010).
8. Mencuccini, M. *et al.* Size-mediated ageing reduces vigour in trees. *Ecol. Lett.* **8,** 1183–1190 (2005).
9. Drake, J. E., Raetz, L. M., Davis, S. C. & DeLucia, E. H. Hydraulic limitation not declining nitrogen availability causes the age-related photosynthetic decline in loblolly pine (*Pinus taeda* L.). *Plant Cell Environ.* **33,** 1756–1766 (2010).
10. Ryan, M. G., Binkley, D. & Fownes, J. H. Age-related decline in forest productivity: pattern and process. *Adv. Ecol. Res.* **27,** 213–262 (1997).
11. Thomas, S. C. in *Size- and Age-Related Changes in Tree Structure and Function* (eds Meinzer, F. C., Lachenbruch, B. & Dawson, T. E.) 33–64 (Springer, 2011).
12. Thomas, H. Senescence, ageing and death of the whole plant. *New Phytol.* **197,** 696–711 (2013).
13. Carey, E. V., Sala, A., Keane, R. & Callaway, R. M. Are old forests underestimated as global carbon sinks? *Glob. Change Biol.* **7,** 339–344 (2001).
14. Phillips, N. G., Buckley, T. N. & Tissue, D. T. Capacity of old trees to respond to environmental change. *J. Integr. Plant Biol.* **50,** 1355–1364 (2008).
15. Piper, F. I. & Fajardo, A. No evidence of carbon limitation with tree age and height in *Nothofagus pumilio* under Mediterranean and temperate climate conditions. *Ann. Bot.* **108,** 907–917 (2011).
16. Weiner, J. & Thomas, S. C. The nature of tree growth and the ''age-related decline in forest productivity''. *Oikos* **94,** 374–376 (2001).
17. Jenkins, J. C., Chojnacky, D. C., Heath, L. S. & Birdsey, R. A. *Comprehensive Database of Diameter-based Biomass Regressions for North American Tree Species* General Technical Report NE-319, http://www.nrs.fs.fed.us/pubs/6725 (USDA Forest Service, Northeastern Research Station, 2004).
18. Niklas, K. J. & Enquist, B. J. Canonical rules for plant organ biomass partitioning and annual allocation. *Am. J. Bot.* **89,** 812–819 (2002).
19. Thomas, S. C. Photosynthetic capacity peaks at intermediate size in temperate deciduous trees. *Tree Physiol.* **30,** 555–573 (2010).
20. Steppe, K., Niinemets, Ü. & Teskey, R. O. in *Size- and Age-Related Changes in Tree Structure and Function* (eds Meinzer, F. C., Lachenbruch, B. & Dawson, T. E.) 235–253 (Springer, 2011).
21. Gilmore, D. W. & Seymour, R. S. Alternative measures of stem growth efficiency applied to *Abies balsamea* from four canopy positions in central Maine, USA. *For. Ecol. Manage.* **84,** 209–218 (1996).
22. Kaufmann, M. R. & Ryan, M. G. Physiographic, stand, and environmental effects on individual tree growth and growth efficiency in subalpine forests. *Tree Physiol.* **2,** 47–59 (1986).
23. Coomes, D. A., Holdaway, R. J., Kobe, R. K., Lines, E. R. & Allen, R. B. A general integrative framework for modelling woody biomass production and carbon sequestration rates in forests. *J. Ecol.* **100,** 42–64 (2012).
24. Binkley, D. A hypothesis about the interaction of tree dominance and stand production through stand development. *For. Ecol. Manage.* **190,** 265–271 (2004).
25. Pretzsch, H. & Biber, P. A re-evaluation of Reineke's rule and stand density index. *For. Sci.* **51,** 304–320 (2005).
26. Kashian, D. M., Turner, M. G., Romme, W. H. & Lorimer, C. G. Variability and convergence in stand structural development on a fire-dominated subalpine landscape. *Ecology* **86,** 643–654 (2005).
27. Munné-Bosch, S. Do perennials really senesce? *Trends Plant Sci.* **13,** 216–220 (2008).
28. Jump, A. S., Hunt, J. M. & Peñuelas, J. Rapid climate change-related growth decline at the southern range edge of *Fagus sylvatica. Glob. Change Biol.* **12,** 2163–2174 (2006).
29. Lindenmayer, D. B., Laurance, W. F. & Franklin, J. F. Global decline in large old trees. *Science* **338,** 1305–1306 (2012).
30. Enquist, B. J., West, G. B. & Brown, J. H. Extensions and evaluations of a general quantitative theory of forest structure and dynamics. *Proc. Natl Acad. Sci. USA* **106,** 7046–7051 (2009).

Supplementary Information is available in the online version of the paper.

Acknowledgements We thank the hundreds of people who have established and maintained the forest plots and their associated databases; M. G. Ryan for comments on the manuscript; C. D. Canham and T. Hart for supplying data; C. D. Canham for discussions and feedback; J. S. Baron for hosting our workshops; and Spain's Ministerio de Agricultura, Alimentación y Medio Ambiente (MAGRAMA) for granting access to the Spanish Forest Inventory Data. Our analyses were supported by the United States Geological Survey (USGS) John Wesley Powell Center for Analysis and Synthesis, the USGS Ecosystems and Climate and Land Use Change mission areas, the Smithsonian Institution Global Earth Observatory—Center for Tropical Forest Science (CTFS), and a University of Nebraska-Lincoln Program of Excellence in Population Biology Postdoctoral Fellowship (to N.G.B.). In addition, X.W. was supported by National Natural Science Foundation of China (31370444) and State Key Laboratory of Forest and Soil Ecology (LFSE2013-11). Data collection was funded by a broad range of organizations including the USGS, the CTFS, the US National Science Foundation, the Andrews LTER (NSF-LTER DEB-0823380), the US National Park Service, the US Forest Service (USFS), the USFS Forest Inventory and Analysis Program, the John D. and Catherine T. MacArthur Foundation, the Andrew W. Mellon Foundation, MAGRAMA, the Council of Agriculture of Taiwan, the National Science Council of Taiwan, the National Natural Science Foundation of China, the Knowledge Innovation Program of the Chinese Academy of Sciences, Landcare Research and the National Vegetation Survey Database (NVS) of New Zealand, the French Fund for the Global Environment and Fundación ProYungas. This paper is a contribution from the Western Mountain Initiative, a USGS global change research project. Any use of trade names is for descriptive purposes only and does not imply endorsement by the USA government.

Author Contributions N.L.S. and A.J.D. conceived the study with feedback from R.C. and D.A.C., N.L.S., A.J.D., R.C. and S.E.R. wrote the manuscript. R.C. devised the main analytical approach and wrote the computer code. N.L.S., A.J.D., R.C., S.E.R., P.J.B., N.G.B., D.A.C., E.R.L., W.K.M. and N.R. performed analyses. N.L.S., A.J.D., R.C., S.E.R., P.J.B., D.A.C., E.R.L., W.K.M., E.Á., C.B., S.B., G.C., S.J.D., Á.D., C.N.E., O.F., J.F.F., H.R.G., Z.H., M.E.H., S.P.H., D.K., Y.L., J.-R.M., A.M., L.R.M., R.J.P., N.P., S.-H.S., I-F.S., S.T., D.T., P.J.v.M., X.W., S.K.W. and M.A.Z. supplied data and sources of allometric equations appropriate to their data.

Author Information Fitted model parameters for each species have been deposited in USGS's ScienceBase at http://dx.doi.org/10.5066/F7JS9NFM. Reprints and permissions information is available at www.nature.com/reprints. The authors declare no competing financial interests. Readers are welcome to comment on the online version of the paper. Correspondence and requests for materials should be addressed to N.L.S. (nstephenson@usgs.gov).

METHODS

Data. We required that forest monitoring plots provided unbiased samples of all living trees within the plot boundaries, and that the trees had undergone two trunk diameter measurements separated by at least one year. Some plots sampled minimally disturbed old (all-aged) forest, whereas others, particularly those associated with national inventories, sampled forest stands regardless of past management history. Plots are described in the references cited in Supplementary Table 1.

Our raw data were consecutive measurements of trunk diameter, D, with most measurements taken 5 to 10 years apart (range, 1–29 years). D was measured at a standard height on the trunk (usually 1.3–1.4 m above ground level), consistent across measurements for a tree. Allometric equations for 16% of species required, in addition to consecutive measurements of D, consecutive measurements of tree height.

We excluded trees exhibiting extreme diameter growth, defined as trunks where D increased by $\geq 40\ \mathrm{mm\ yr^{-1}}$ or that shrank by $\geq 12s$, where s is the standard deviation of the D measurement error, $s = 0.9036 + 0.006214D$ (refs 31, 32); outliers of these magnitudes were almost certainly due to error. By being so liberal in allowing negative growth anomalies, we erred on the side of reducing our ability to detect increases in tree mass growth rate. Using other exclusion values yielded similar results, as did a second approach to handling error in which we reanalysed a subset of our models using a Bayesian method that estimates growth rates after accounting for error, based on independent plot-specific data quantifying measurement error[33].

To standardize minimum D among data sets, we analysed only trees with $D \geq 10$ cm at the first census. To ensure adequate samples of trees spanning a broad range of sizes, we restricted analyses to species having both ≥ 40 trees in total and also ≥ 15 trees with $D \geq 30$ cm at the first census. This left us with 673,046 trees belonging to 403 tropical and temperate species in 76 families, spanning twelve countries and all forested continents (Supplementary Table 1). Maximum trunk diameters ranged from 38 cm to 270 cm among species, and averaged 92 cm.

Estimating tree mass. To estimate each tree's aboveground dry mass, M, we used published allometric equations relating M to D (or for 16% of species, relating M to D and tree height). Some equations were species-specific and others were specific to higher taxonomic levels or forest types, described in the references in Supplementary Table 1. The single tropical moist forest equation of ref. 34 was applied to most tropical species, whereas most temperate species had unique species-specific equations. Most allometric equations are broadly similar, relating $\log(M)$ to $\log(D)$ linearly, or nearly linearly—a familiar relationship in allometric scaling of both animals and plants[35]. Equations can show a variety of differences in detail, however, with some adding $\log(D)$ squared and cubed terms. All equations make use of the wood density of individual species, but when wood density was not available for a given species we used mean wood density for a genus or family[36].

Using a single, average allometry for most tropical species, and mean wood density for a genus or family for several species, limits the accuracy of our estimates of M. However, because we treat each species separately, it makes no difference whether our absolute M estimates are more accurate in some species than in others, only that they are consistent within a species and therefore accurately reveal whether mass growth rates increase or decrease with tree size.

For two regions—Spain and the western USA—allometric equations estimated mass only for a tree's main stem rather than all aboveground parts, including branches and leaves. But because leaf and stem masses are positively correlated and their growth rates are expected to scale isometrically both within and among species[18,37,38], results from these two regions should not alter our qualitative conclusions. Confirming this, the percentage of species with increasing stem mass growth rate in the last bin for Spain and the western USA (93.4% of 61 species) was similar to that from the remainder of regions (97.4% of 342 species) ($P = 0.12$, Fisher's exact test).

Modelling mass growth rate. We sought a modelling approach that made no assumptions about the shape of the relationship between aboveground dry mass growth rate, G, and aboveground dry mass, M, and that could accommodate monotonically increasing, monotonically decreasing, or hump-shaped relationships. We therefore chose to model G as a function of $\log(M)$ using piecewise linear regression. The range of the x axis, $X = \log(M)$, is divided into a series of bins, and within each bin G is fitted as a function of X by linear regression. The position of the bins is adaptive: it is fitted along with the regression terms. Regression lines are required to meet at the boundary between bins. For a single model-fitting run the number of bins, B, is fixed. For example, if $B = 2$, there are four parameters to be fitted for a single species: the location of the boundary between bins, X_1; the slope of the regression in the first bin, S_1; the slope in the second bin, S_2; and an intercept term. Those four parameters completely define the model. In general, there are $2B$ parameters for B bins.

Growth rates, while approximately normally distributed, were heteroskedastic, with the variance increasing with mass (Fig. 1), so an additional model was needed for the standard deviation of G, σ_G, as a function of $\log(M)$. The increase of σ_G with $\log(M)$ was clearly not linear, so we used a three-parameter model:

$$\sigma_G = k \qquad (\text{for } \log(M) < d)$$

$$\sigma_G = a + b\log(M) \qquad (\text{for } \log(M) \geq d)$$

where the intercept a is determined by the values of k, d and b. Thus σ_G was constant for smaller values of $\log(M)$ (below the cutoff d), then increased linearly for larger $\log(M)$ (Fig. 1). The parameters k, d and b were estimated along with the parameters of the growth model.

Parameters of both the growth and standard deviation models were estimated in a Bayesian framework using the likelihood of observing growth rates given model predictions and the estimated standard deviation of the Gaussian error function. A Markov chain Monte Carlo chain of parameter estimates was created using a Gibbs sampler with a Metropolis update[39,40] written in the programming language R (ref. 41) (a tutorial and the computer code are available through http://ctfs.arnarb.harvard.edu/Public/CTFSRPackage/files/tutorials/growthfitAnalysis). The sampler works by updating each of the parameters in sequence, holding other parameters fixed while the relevant likelihood function is used to locate the target parameter's next value. The step size used in the updates was adjusted adaptively through the runs, allowing more rapid convergence[40]. The final Markov chain Monte Carlo chain describes the posterior distribution for each model parameter, the error, and was then used to estimate the posterior distribution of growth rates as estimated from the model. Priors on model parameters were uniform over an unlimited range, whereas the parameters describing the standard deviation were restricted to >0. Bin boundaries, X_i, were constrained as follows: (1) boundaries could only fall within the range of X, (2) each bin contained at least five trees, and (3) no bin spanned less than 10% of the range of X. The last two restrictions prevented the bins from collapsing to very narrow ranges of X in which the fitted slope might take absurd extremes.

We chose piecewise regression over other alternatives for modelling G as a function of M for two main reasons. First, the linear regression slopes within each bin provide precise statistical tests of whether G increases or decreases with X, based on credible intervals of the slope parameters. Second, with adaptive bin positions, the function is completely flexible in allowing changes in slope at any point in the X range, with no influence of any one bin on the others. In contrast, in parametric models where a single function defines the relationship across all X, the shape of the curve at low X can (and indeed must) influence the shape at high X, hindering statistical inference about changes in tree growth at large size.

We used $\log(M)$ as our predictor because within a species M has a highly non-Gaussian distribution, with many small trees and only a few very large trees, including some large outliers. In contrast, we did not log-transform our dependent variable G so that we could retain values of $G \leq 0$ that are often recorded in very slowly growing trees, for which diameter change over a short measurement interval can be on a par with diameter measurement error.

For each species, models with 1, 2, 3 and 4 bins were fitted. Of these four models, the model receiving the greatest weight of evidence by Akaike Information Criterion (AIC) was selected. AIC is defined as the log-likelihood of the best-fitting model, penalized by twice the number of parameters. Given that adding one more bin to a model meant two more parameters, the model with an extra bin had to improve the log-likelihood by 4 to be considered a better model[42].

Assessing model fits. To determine whether our approach might have failed to reveal a final growth decline within the few largest trees of the various species, we calculated mass growth rate residuals for the single most massive individual tree of each species. For 52% of the 403 species, growth of the most massive tree was underestimated by our model fits (for example, Fig. 1a); for 48% it was overestimated (for example, Fig. 1b). These proportions were indistinguishable from 50% ($P = 0.55$, binomial test), as would be expected for unbiased model fits. Furthermore, the mean residual (observed minus predicted) mass growth rate of these most massive trees, $+0.006\ \mathrm{Mg\ yr^{-1}}$, was statistically indistinguishable from zero ($P = 0.29$, two-tailed t-test). We conclude that our model fits accurately represent growth trends up through, and including, the most massive trees.

Effects of combined data. To achieve sample sizes adequate for analysis, for some species we combined data from several different forest plots, potentially introducing a source of bias: if the largest trees of a species disproportionately occur on productive sites, the increase in mass growth rate with tree size could be exaggerated. This might occur because trees on less-productive sites—presumably the sites having the slowest-growing trees within any given size class—could be underrepresented in the largest size classes. We assessed this possibility in two ways.

First, our conclusions remained unchanged when we compared results for the 53% of species that came uniquely from single large plots with those of the 47% of species whose data were combined across several plots. Proportions of species with increasing mass growth rates in the last bin were indistinguishable between the two groups (97.6% and 95.8%, respectively; $P = 0.40$, Fisher's exact test). Additionally,

the shapes and magnitudes of the growth curves for Africa and Asia, where data for each species came uniquely from single large plots, were similar to those of Australasia, Europe and North America, where data for each species were combined across several plots (Table 1, Fig. 2 and Extended Data Fig. 2). (Data from Central and South America were from both single and combined plots, depending on species.)

Second, for a subset of combined-data species we compared two sets of model fits: (1) using all available plots (that is, the analyses we present in the main text), and (2) using only plots that contained massive trees—those in the top 5% of mass for a species. To maximize our ability to detect differences, we limited these analyses to species with large numbers of trees found in a large number of plots, dispersed widely across a broad geographic region. We therefore analysed the twelve Spanish species that each had more than 10,000 individual trees (Supplementary Table 1), found in 34,580 plots distributed across Spain. Massive trees occurred in 6,588 (19%) of the 34,580 plots. We found no substantial differences between the two analyses. When all 34,580 plots were analysed, ten of the twelve species showed increasing growth in the last bin, and seven showed increasing growth across all bins; when only the 6,588 plots containing the most massive trees were analysed, the corresponding numbers were eleven and nine. Model fits for the two groups were nearly indistinguishable in shape and magnitude across the range of tree masses. We thus found no evidence that the potential for growth differences among plots influenced our conclusions.

Effects of possible allometric biases. For some species, the maximum trunk diameter D in our data sets exceeded the maximum used to calibrate the species' allometric equation. In such cases our estimates of M extrapolate beyond the fitted allometry and could therefore be subject to bias. For 336 of our 403 species we were able to determine D of the largest tree that had been used in calibrating the associated allometric equations. Of those 336 species, 74% (dominated by tropical species) had no trees in our data set with D exceeding that used in calibrating the allometric equations, with the remaining 26% (dominated by temperate species) having at least one tree with D exceeding that used in calibration. The percentage of species with increasing G in the last bin for the first group (98.0%) was indistinguishable from that of the second group (96.6%) ($P = 0.44$, Fisher's exact test). Thus, our finding of increasing G with tree size is not affected by the minority of species that have at least one tree exceeding the maximum value of D used to calibrate their associated allometric equations.

A bias that could inflate the rate at which G increases with tree size could arise if allometric equations systematically underestimate M for small trees or overestimate M for large trees[43]. For a subset of our study species we obtained the raw data—consisting of measured values of D and M for individual trees—needed to calibrate allometric equations, allowing us to determine whether the particular form of those species' allometric equations was prone to bias, and if so, the potential consequences of that bias.

To assess the potential for allometric bias for the majority (58%) of species in our data set—those that used the empirical moist tropical forest equation of ref. 34—we reanalysed the data provided by ref. 34. The data were from 1,504 harvested trees representing 60 families and 184 genera, with D ranging from 5 cm to 156 cm; the associated allometric equation relates $\log(M)$ to a third-order polynomial of $\log(D)$. Because the regression of M on D was fitted on a log–log scale, this and subsequent equations include a correction of $\exp[(\mathrm{RSE})^2/2]$ for the error in back-transformation, where RSE is the residual standard error from the statistical model[44]. Residuals of M for the equation revealed no evident biases (Extended Data Fig. 4a), suggesting that we should expect little (if any) systematic size-related biases in our estimates of G for the 58% of our species that used this equation.

Our simplest form of allometric equation—applied to 22% of our species—was $\log(M) = a + b\log(D)$, where a and b are taxon-specific constants. For nine of our species that used equations of this form (all from the temperate western USA: *Abies amabilis, A. concolor, A. procera, Pinus lambertiana, Pinus ponderosa, Picea sitchensis, Pseudotsuga menziesii, Tsuga heterophylla* and *T. mertensiana*) we had values of both D and M for a total of 1,358 individual trees, allowing us to fit species-specific allometric equations of the form $\log(M) = a + b\log(D)$ and then assess them for bias. Residual plots showed a tendency to overestimate M for the largest trees (Extended Data Fig. 4b), with the possible consequence of inflating estimates of G for the largest relative to the smallest trees of these species.

To determine whether this bias was likely to alter our qualitative conclusion that G increases with tree size, we created a new set of allometric relations between D and M —one for each of the nine species—using the same piecewise linear regression approach we used to model G as a function of M. However, because our goal was to eliminate bias rather than seek the most parsimonious model, we fixed the number of bins at four, with the locations of boundaries between the bins being fitted by the model. Our new allometry using piecewise regressions led to predictions of M with no apparent bias relative to D (Extended Data Fig. 4c). This new, unbiased allometry gave the same qualitative results as our original, simple allometry regarding the relationship between G and M: for all nine species, G increased in the bin containing the largest trees, regardless of the allometry used (Extended Data Fig. 5). We conclude that any bias associated with the minority of our species that used the simple allometric equation form was unlikely to affect our broad conclusion that G increases with tree size in a majority of tree species.

As a final assessment, we compared our results to those of a recent study of *E. regnans* and *S. sempervirens*, in which M and G had been calculated from intensive measurements of aboveground portions of trees without the use of standard allometric equations[7]. Specifically, in two consecutive years 36 trees of different sizes and ages were climbed, trunk diameters were systematically measured at several heights, branch diameters and lengths were measured (with subsets of foliage and branches destructively sampled to determine mass relationships), wood densities were determined and ring widths from increment cores were used to supplement measured diameter growth increments. The authors used these measurements to calculate M for each of the trees in each of the two consecutive years, and G as the difference in M between the two years[7]. *E. regnans* and *S. sempervirens* are the world's tallest angiosperm and gymnosperm species, respectively, so the data set was dominated by exceptionally large trees; most had $M \geq 20$ Mg, and M of some individuals exceeded that of the most massive trees in our own data set (which lacked *E. regnans* and *S. sempervirens*). We therefore compared *E. regnans* and *S. sempervirens* to the 58 species in our data set that had at least one individual with $M \geq 20$ Mg. Sample sizes for *E. regnans* and *S. sempervirens*—15 and 21 trees, respectively—fell below our required ≥40 trees for fitting piecewise linear regressions, so we simply plotted data points for individual *E. regnans* and *S. sempervirens* along with the piecewise regressions that we had already fitted for our 58 comparison species (Fig. 3).

As reported by ref. 7, G increased with M for both *E. regnans* and *S. sempervirens*, up to and including some of the most massive individual trees on the Earth (Fig. 3). Within the zone of overlapping M between the two data sets, G values for individual *E. regnans* and *S. sempervirens* trees fell almost entirely within the ranges of the piecewise regressions we had fitted for our 58 comparison species. We take these observations as a further indication that our results, produced using standard allometric equations, accurately reflect broad relationships between M and G.

Fitting log–log models. To model $\log(G)$ as a function of $\log(M)$, we used the binning approach that we used in our primary analysis of mass growth rate (described earlier). However, in log-transforming growth we dropped trees with $G \leq 0$. Because negative growth rates become more extreme with increasing tree size, dropping them could introduce a bias towards increasing growth rates. Log-transformation additionally resulted in skewed growth rate residuals. Dropping trees with $G \leq 0$ caused several species to fall below our threshold sample size, reducing the total number of species analysed to 381 (Extended Data Fig. 2).

Growth in the absence of competition. We obtained published equations for 41 North American and European species, in 46 species-site combinations, relating species-specific tree diameter growth rates to trunk diameter D and to neighbourhood competition[45–49]. Setting neighbourhood competition to zero gave us equations describing estimated annual D growth as a function of D in the absence of competition. Starting at $D_0 = 10$ cm, we sequentially (1) calculated annual D growth for a tree of size D_t, (2) added this amount to D_t to determine D_{t+1}, (3) used an appropriate taxon-specific allometric equation to calculate the associated tree masses M_t and M_{t+1}, and (iv) calculated tree mass growth rate G_t of a tree of mass M_t in the absence of competition as $M_{t+1} - M_t$. For each of the five species that had separate growth analyses available from two different sites, we required that mass growth rate increased continuously with tree size at both sites for the species to be considered to have a continuously increasing mass growth rate. North American and European allometries were taken from refs 17 and 50, respectively, with preference given to allometric equations based on power functions of tree diameter, large numbers of sampled trees, and trees spanning a broad range of diameters. For the 47% of European species for which ref. 50 had no equations meeting our criteria, we used the best-matched (by species or genus) equations from ref. 17.

31. Condit, R. *et al.* Tropical forest dynamics across a rainfall gradient and the impact of an El Niño dry season. *J. Trop. Ecol.* **20,** 51–72 (2004).
32. Condit, R. *et al.* The importance of demographic niches to tree diversity. *Science* **313,** 98–101 (2006).
33. Rüger, N., Berger, U., Hubbell, S. P., Vieilledent, G. & Condit, R. Growth strategies of tropical tree species: disentangling light and size effects. *PLoS ONE* **6,** e25330 (2011).
34. Chave, J. *et al.* Tree allometry and improved estimation of carbon stocks and balance in tropical forests. *Oecologia* **145,** 87–99 (2005).
35. Sibly, R. M., Brown, J. H. & Kodric-Brown, A. (eds) *Metabolic Ecology: A Scaling Approach* (John Wiley & Sons, 2012).
36. Zanne, A. E. *et al.* Data from: Towards a worldwide wood economics spectrum. In *Dryad Digital Data Repository*, http://dx.doi.org/10.5061/dryad.234 (2009).
37. Enquist, B. J. & Niklas, K. J. Global allocation rules for patterns of biomass partitioning in seed plants. *Science* **295,** 1517–1520 (2002).

38. Niklas, K. J. Plant allometry: is there a grand unifying theory? *Biol. Rev.* **79,** 871–889 (2004).
39. Metropolis, N., Rosenbluth, A. W., Rosenbluth, M. N., Teller, A. H. & Teller, E. Equation of state calculations by fast computing machines. *J. Chem. Phys.* **21,** 1087–1092 (1953).
40. Rüger, N., Huth, A., Hubbell, S. P. & Condit, R. Determinants of mortality across a tropical lowland rainforest community. *Oikos* **120,** 1047–1056 (2011).
41. R Development Core Team. *R: A Language and Environment for Statistical Computing* (R Foundation for Statistical Computing, 2009).
42. Hilborn, R. & Mangel, M. *The Ecological Detective: Confronting Models with Data* (Princeton Univ. Press, 1997).
43. Chambers, J. Q., Dos Santos, J., Ribeiro, R. J. & Higuchi, N. Tree damage, allometric relationships, and above-ground net primary production in central Amazon forest. *For. Ecol. Manage.* **152,** 73–84 (2001).
44. Baskerville, G. L. Use of logarithmic regression in the estimation of plant biomass. *Can. J. For. Res.* **2,** 49–53 (1972).
45. Canham, C. D. *et al.* Neighborhood analyses of canopy tree competition along environmental gradients in New England forests. *Ecol. Appl.* **16,** 540–554 (2006).
46. Coates, K. D., Canham, C. D. & LePage, P. T. Above- versus below-ground competitive effects and responses of a guild of temperate tree species. *J. Ecol.* **97,** 118–130 (2009).
47. Pretzsch, H. & Biber, P. Size-symmetric versus size-asymmetric competition and growth partitioning among trees in forest stands along an ecological gradient in central Europe. *Can. J. For. Res.* **40,** 370–384 (2010).
48. Gómez-Aparicio, L., García-Valdés, R., Ruíz-Benito, P. & Zavala, M. A. Disentangling the relative importance of climate, size and competition on tree growth in Iberian forests: implications for forest management under global change. *Glob. Change Biol.* **17,** 2400–2414 (2011).
49. Das, A. The effect of size and competition on tree growth rate in old-growth coniferous forests. *Can. J. For. Res.* **42,** 1983–1995 (2012).
50. Zianis, D., Muukkonen, P., Makipaa, R. & Mencuccini, M. Biomass and stem volume equations for tree species in Europe. *Silva Fennica Monogr.* **4,** 1–63 (2005).

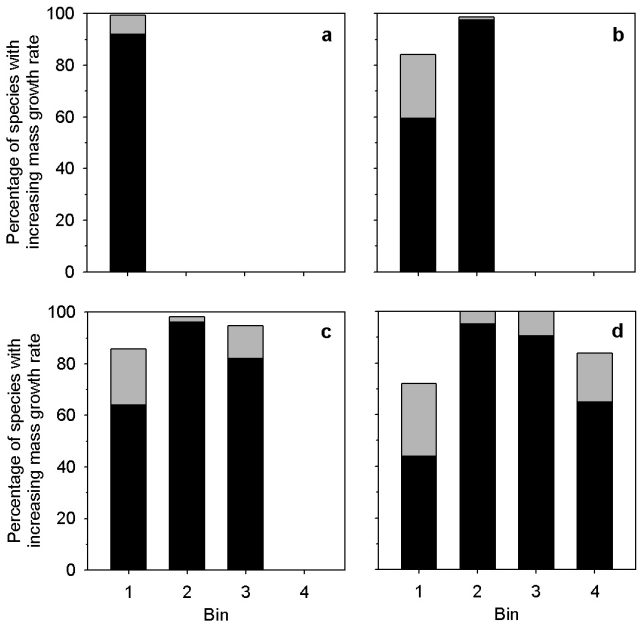

Extended Data Figure 1 | Summary of model fits for tree mass growth rates. Bars show the percentage of species with mass growth rates that increase with tree mass for each bin; black shading indicates percentage significant at $P \leq 0.05$. Tree masses increase with bin number. **a**, Species fitted with one bin (165 species); **b**, Species fitted with two bins (139 species); **c**, Species fitted with three bins (56 species); and **d**, Species fitted with four bins (43 species).

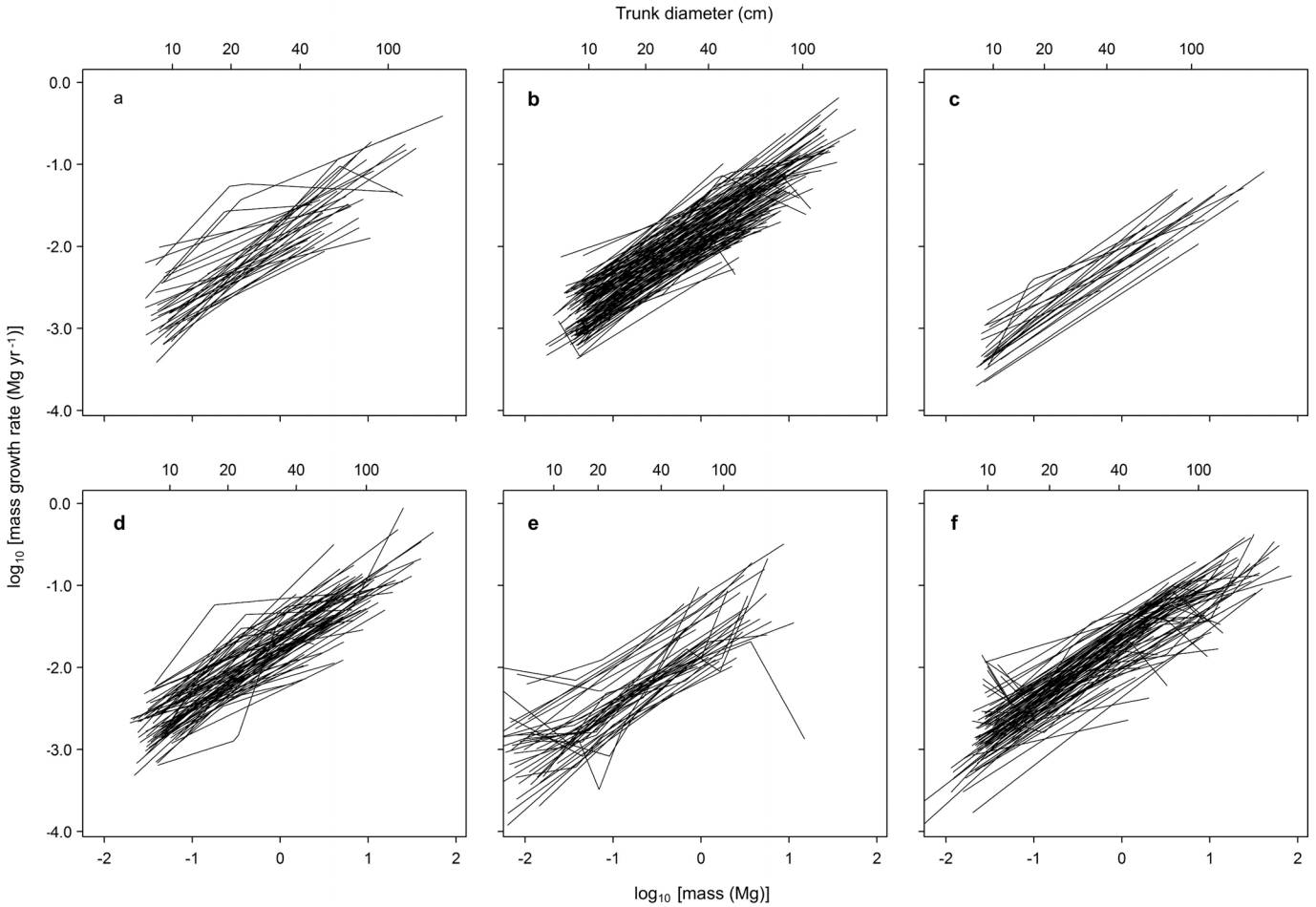

Extended Data Figure 2 | Log–log model fits of mass growth rates for 381 tree species, by continent. Trees with growth rates ≤ 0 were dropped from the analysis, reducing the number of species meeting our threshold sample size for analysis. **a**, Africa (33 species); **b**, Asia (123 species); **c**, Australasia (22 species); **d**, Central and South America (73 species); **e**, Europe (41 species); and **f**, North America (89 species). Trunk diameters are approximate values for reference, based on the average diameters of trees of a given mass.

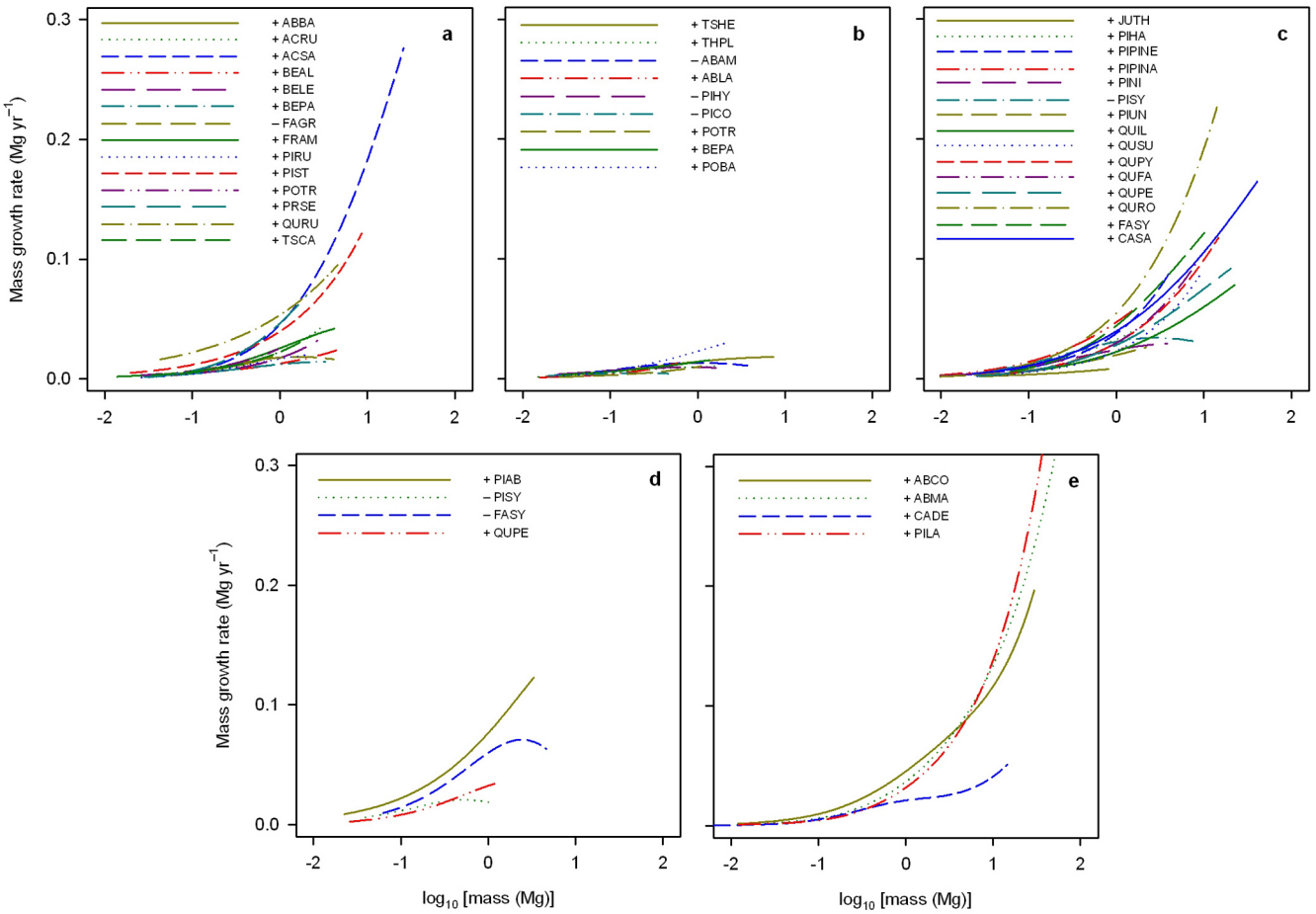

Extended Data Figure 3 | Aboveground mass growth rates for 41 tree species in the absence of competition. The '+' or '−' symbol preceding each species code indicates, respectively, species with mass growth rates that increased continuously with tree size or species with mass growth rates that declined in the largest trees. Sources of the diameter growth equations used to calculate mass growth were: **a**, ref. 45; **b**, ref. 46; **c**, ref. 48; **d**, ref. 47; and **e**, ref. 49. ABAM, *Abies amabilis*; ABBA, *Abies balsamea*; ABCO, *Abies concolor*; ABLA, *Abies lasiocarpa*; ABMA, *Abies magnifica*; ACRU, *Acer rubrum*; ACSA, *Acer saccharum*; BEAL, *Betula alleghaniensis*; BELE, *Betula lenta*; BEPA, *Betula papyrifera*; CADE, *Calocedrus decurrens*; CASA, *Castanea sativa*; FAGR, *Fagus grandifolia*; FASY, *Fagus sylvatica*; FRAM, *Fraxinus americana*; JUTH, *Juniperus thurifera*; PIAB, *Picea abies*; PICO, *Pinus contorta*; PIHA, *Pinus halepensis*; PIHY, *Picea* hybrid (a complex of *Picea glauca*, *P. sitchensis* and *P. engelmannii*); PILA, *Pinus lambertiana*; PINI, *Pinus nigra*; PIPINA, *Pinus pinaster*; PIPINE, *Pinus pinea*; PIRU, *Picea rubens*; PIST, *Pinus strobus*; PISY, *Pinus sylvestris*; PIUN, *Pinus uncinata*; POBA, *Populus balsamifera* ssp. *trichocarpa*; POTR, *Populus tremuloides*; PRSE, *Prunus serotina*; QUFA, *Quercus faginea*; QUIL, *Quercus ilex*; QUPE, *Quercus petraea*; QUPY, *Quercus pyrenaica*; QURO, *Quercus robar*; QURU, *Quercus rubra*; QUSU, *Quercus suber*; THPL, *Thuja plicata*; TSCA, *Tsuga canadensis*; and TSHE, *Tsuga heterophylla*.

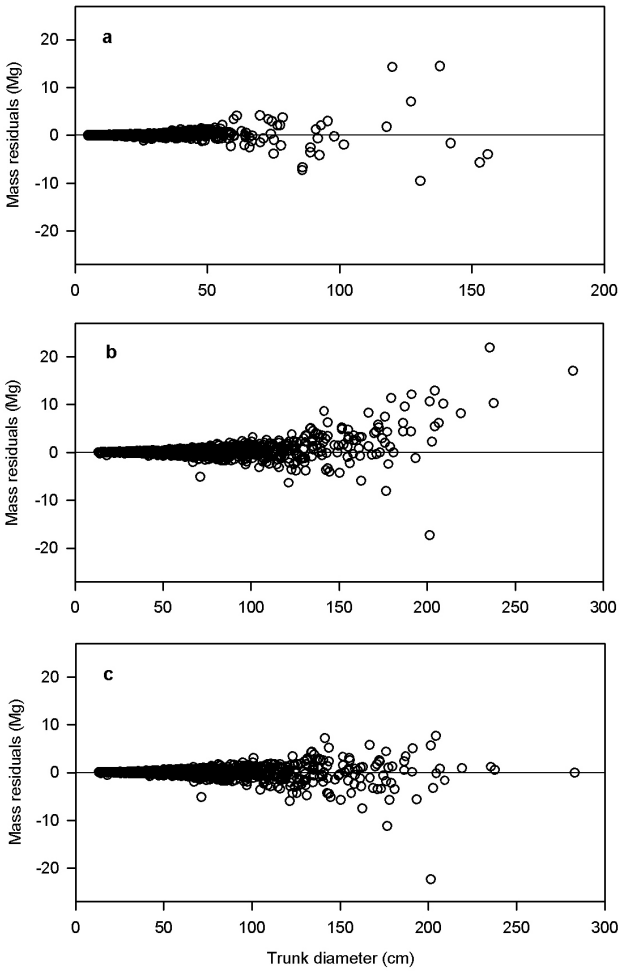

Extended Data Figure 4 | Residuals of predicted minus observed tree mass. **a**, The allometric equation for moist tropical forests[34]—used for the majority of tree species—shows no evident systematic bias in predicted aboveground dry mass, *M*, relative to trunk diameter ($n = 1{,}504$ trees). **b**, In contrast, our simplest form of allometric equation—used for 22% of our species and here applied to nine temperate species—shows an apparent bias towards overestimating *M* for large trees ($n = 1{,}358$ trees). **c**, New allometries that we created for the nine temperate species removed the apparent bias in predicted *M*.

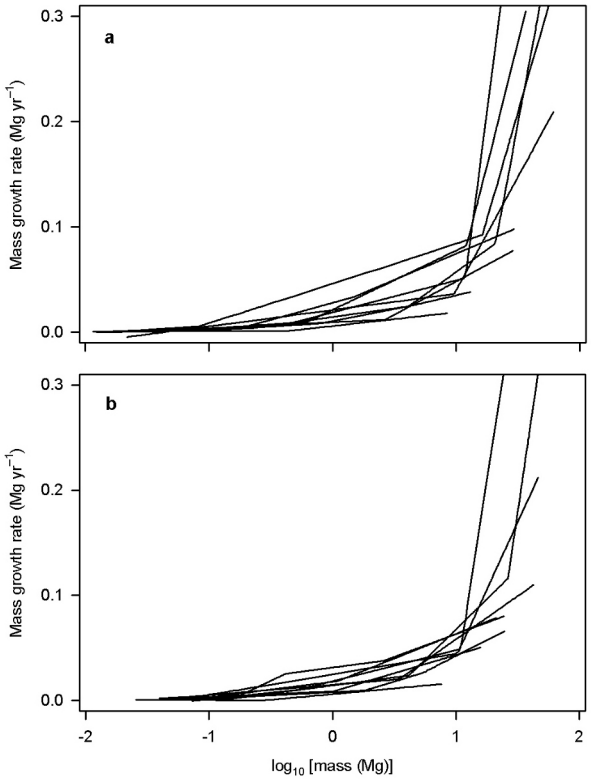

Extended Data Figure 5 | Estimated mass growth rates of the nine temperate species of Extended Data Fig. 4. Growth was estimated using the simplest form of allometric model [$\log(M) = a + b\log(D)$] (**a**) and our allometric models fitted with piecewise linear regression (**b**). Regardless of the allometric model form, all nine species show increasing G in the largest trees.